

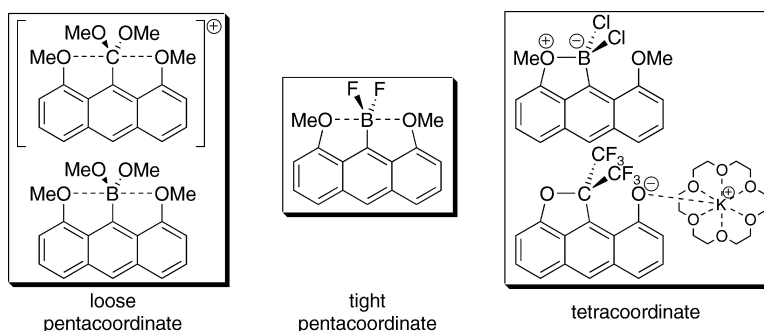
Article

# Syntheses and Structures of Hypervalent Pentacoordinate Carbon and Boron Compounds Bearing an Anthracene Skeleton – Elucidation of Hypervalent Interaction Based on X-ray Analysis and DFT Calculation

Makoto Yamashita, Yohsuke Yamamoto, Kin-ya Akiba, Daisuke Hashizume, Fujiko Iwasaki, Nozomi Takagi, and Shigeru Nagase

*J. Am. Chem. Soc.*, **2005**, 127 (12), 4354-4371 • DOI: 10.1021/ja0438011 • Publication Date (Web): 05 March 2005

Downloaded from <http://pubs.acs.org> on March 24, 2009



## More About This Article

Additional resources and features associated with this article are available within the HTML version:

- Supporting Information
- Links to the 16 articles that cite this article, as of the time of this article download
- Access to high resolution figures
- Links to articles and content related to this article
- Copyright permission to reproduce figures and/or text from this article

[View the Full Text HTML](#)

## Syntheses and Structures of Hypervalent Pentacoordinate Carbon and Boron Compounds Bearing an Anthracene Skeleton – Elucidation of Hypervalent Interaction Based on X-ray Analysis and DFT Calculation

Makoto Yamashita,<sup>†</sup> Yohsuke Yamamoto,<sup>\*,†</sup> Kin-ya Akiba,<sup>\*,‡</sup> Daisuke Hashizume,<sup>§</sup>  
Fujiko Iwasaki,<sup>§</sup> Nozomi Takagi,<sup>||</sup> and Shigeru Nagase<sup>||</sup>

Contribution from the Department of Chemistry, Graduate School of Science, Hiroshima University, 1-3-1 Kagamiyama, Higashi-Hiroshima 739-8526, Japan, Advanced Research Center for Science and Engineering, Waseda University, 3-4-1 Ohkubo, Shinjuku-ku, Tokyo 165-8555, Japan, Department of Applied Physics and Chemistry, The University of Electro-Communications, 1-5-1 Chofugaoka, Chofu, Tokyo 182-8585, Japan, and Department of Theoretical Molecular Science, Institute for Molecular Science, Myodaiji, Okazaki 444-8585, Japan

Received November 30, 2004; E-mail: yyama@sci.hiroshima-u.ac.jp; akibaky@waseda.jp

**Abstract:** Pentacoordinate and tetracoordinate carbon and boron compounds (**27**, **38**, **50–52**, **56–61**) bearing an anthracene skeleton with two oxygen or nitrogen atoms at the 1,8-positions were synthesized by the use of four newly synthesized tridentate ligand precursors. Several carbon and boron compounds were characterized by X-ray crystallographic analysis, showing that compounds **27**, **56–59** bearing an oxygen-donating anthracene skeleton had a trigonal bipyramidal (TBP) pentacoordinate structure with relatively long apical distances (ca. 2.38–2.46 Å). Despite the relatively long apical distances, DFT calculation of carbon species **27** and boron species **56** and experimental accurate X-ray electron density distribution analysis of **56** supported the existence of the apical hypervalent bond even though the nature of the hypervalent interaction between the central carbon (or boron) and the donating oxygen atom was relatively weak and ionic. On the other hand, X-ray analysis of compounds **50–52** bearing a nitrogen-donating anthracene skeleton showed unsymmetrical tetracoordinate carbon or boron atom with coordination by only one of the two nitrogen-donating groups. It is interesting to note that, with an oxygen-donating skeleton, the compound **61** having two chlorine atoms on the central boron atom showed a tetracoordinate structure, although the corresponding compound **60** with two fluorine atoms showed a pentacoordinate structure. The B–O distances (av 2.29 Å) in **60** were relatively short in comparison with those (av 2.44 Å) in **59** having two methoxy groups on the central boron atom, indicating that the B–O interaction became stronger due to the electron-withdrawing nature of the fluorine atoms.

### Introduction

Pentacoordinate carbon compounds should be classified into electron-deficient and electron-rich species based on the number of formal valence electrons around the central carbon. Electron-deficient pentacoordinate carbon compounds such as methonium ion ( $\text{CH}_5^+$ ),<sup>1</sup> transition-metal complexes bearing C–H agostic

interaction or bridging alkyl groups,<sup>2</sup> carboranes,<sup>3</sup> and a carbon atom in a metal cluster cage<sup>4</sup> have eight electrons formally assignable around the central carbon, and the pentacoordinate structure is made possible by the interaction between a  $\sigma$  bond (two-center two-electron bond: 2c-2e) with a vacant orbital of proton and so forth. In contrast, electron-rich pentacoordinate carbon species such as the transition states of the  $\text{S}_{\text{N}}2$  reaction have 10 electrons formally assignable around the central carbon atom based on an interaction of a vacant 2p orbital of the central carbon atom with two lone-pair electrons (four electrons) or an interaction between a vacant C–X  $\sigma^*$  orbital and a lone pair of a nucleophile. The interaction leads to the formation of a linear three-center four-electron (3c-4e) “hypervalent”<sup>5</sup> bonding system; thus, they are called hypervalent compounds.

Theoretical calculations showed that the transition state of the  $\text{S}_{\text{N}}2$  reaction should be  $D_{3h}$  trigonal bipyramidal (TBP). In some cases, the pentacoordinate carbon species could be found

<sup>†</sup> Hiroshima University.

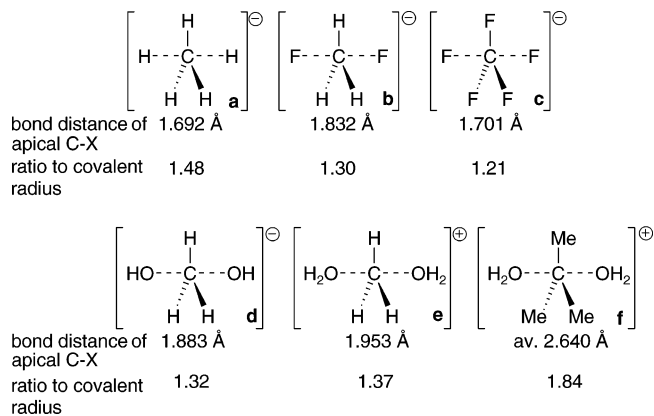
<sup>‡</sup> Waseda University.

<sup>§</sup> The University of Electro-Communications.

<sup>||</sup> Institute for Molecular Science.

(1) Methonium ion ( $\text{CH}_5^+$ ): (a) Olah, G. A.; Laali, K. K.; Wang, Q.; Prakash, G. K. S. *Onium Ions*; John Wiley & Sons: New York, 1998. (b) Olah, G. A.; Prakash, G. K. S.; Williams, R. E.; Field, L. D.; Wade, K. *Hypercarbon Chemistry*; John Wiley & Sons: New York, 1987. (c) Olah, G. A.; Prakash, G. K. S.; Sommer, J. *Superacids*; John Wiley & Sons: New York, 1985. (d) Marx, D.; Parrinello, M. *Nature* **1995**, *375*, 216–218. (e) Schreiner, P. R.; Kim, S.-J.; Schaefer, H. F.; Schleyer, P. v. R. *J. Chem. Phys.* **1993**, *99*, 3716–3720. (f) Scuseria, G. E. *Nature*, **1993**, *366*, 512–513. (g) Olah, G. A.; Klopman, G.; Schlosberg, R. H. *J. Am. Chem. Soc.* **1969**, *91*, 3261–3268.

as the transition state of the solvent-exchange process of solvated carbocations.<sup>6a,b</sup> The transition-state structures of S<sub>N</sub>2 reactions such as CH<sub>3</sub><sup>-</sup> (**a**), CH<sub>3</sub>F<sub>2</sub><sup>-</sup> (**b**), CF<sub>5</sub><sup>-</sup> (**c**), CH<sub>3</sub>(OH)<sub>2</sub><sup>-</sup> (**d**), CH<sub>3</sub><sup>-</sup>(OH)<sub>2</sub><sup>+</sup> (**e**), and CMe<sub>3</sub>(OH)<sub>2</sub><sup>+</sup> (**f**) or solvent exchange S<sub>N</sub>2-like processes of the solvated carbocations under S<sub>N</sub>1 conditions are illustrated together with the ratio of the calculated apical C–X distance to the sum of the covalent radii<sup>7</sup> (Figure 1). All of these imaginary molecules are built up from an sp<sup>2</sup> carbocation coordinated by two anionic nucleophiles (**a–d**) and by two neutral nucleophiles (**e, f**). The two linear hypervalent apical bonds are relatively long (dotted lines in Figure 1). The elongation of apical bonds compared to sp<sup>2</sup> equatorial bonds is widely found in hypervalent compounds of main group elements such as phosphorus, sulfur, silicon, and so forth. Based on comparison of **a, b**, and **d**, it is seen that the apical bond elongation should be related with the electronegativity and hence the atomic radius of apical X. In the case of **b** and **c**, equatorial fluorine atoms made the C–F apical bond shorter. In the case of **d, e**, and **f**, the C–O bond in **e** and **f** was elongated in comparison with **d** probably due to the decrease in nucleophilicity of the neutral nucleophiles (H<sub>2</sub>O) compared with the



**Figure 1.** Calculated hypervalent pentacoordinate carbon structures for transition state of S<sub>N</sub>2.

hydroxide ion and to the presence of the cationic charge in **e** and **f**. By comparison of **e** and **f**, it is apparent that the equatorial methyl group elongates the apical C–O bond. Thus, theoretical calculations have provided information about the structures of pentacoordinate carbon species including substituent effects on the structure.

However, there have been no reliable experimental investigations before us about the structural and bonding features of pentacoordinate carbon species because of the difficulties in synthesizing appropriate model compounds. In addition, there have been only few examples of the theoretical investigation about hypervalent pentacoordinate boron compounds which are isoelectronic to carbocations. The hypervalent boron compound was assumed as a transition state of the S<sub>N</sub>2-type reaction on the central boron atom of a borane–carbon monoxide complex with trimethylamine by the Grotewold group.<sup>8</sup> In 1995, the Oki group reported the direct observation of intramolecular S<sub>N</sub>2 displacement reactions using a 2,6-disubstituted benzene ligand.<sup>9</sup> However, the details of the structure and nature of the transition state have never been studied after Grotewold's assumption.

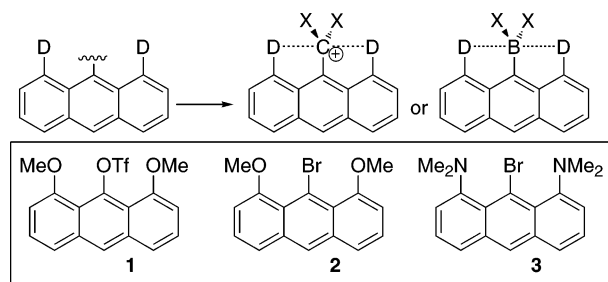
Some chemists have confronted the very difficult problem of the synthesis of stabilized hypervalent carbon and boron compounds. Breslow challenged the problem using trityl cation derivatives bearing some *o*-methylthiomethyl substituents as early as 1966.<sup>10</sup> The compound came out as sulfonium salts, and they could not find any positive evidence for the presence of pentacoordinate carbon compounds. Martin and Basalay attempted to stabilize the pentacoordinate carbon species by the 1,8-bis(phenylthio)anthracenyl ligand.<sup>11</sup> At room temperature, the peak of two methyl groups on the carbocation attached at C-9 was observed as a singlet. When the temperature was lowered, two singlet peaks of the two methyl groups were observed because of the formation of a sulfonium salt, where one of the phenylthio groups stays unaffected. They concluded that the desired pentacoordinate carbon species should be the transition state in the “bell-clapper” (bond-switching) rearrange-

- (2) agostic interaction or bridging alkyl groups: (a) Braunstein, P.; Boag, N. *M. Angew. Chem., Int. Ed.* **2001**, *40*, 2427–2433 and references therein. (b) Boesveld, W. M.; Hitchcock, P. B.; Lappert, M. F.; Liu, D. S.; Tian, S. *Organometallics* **2000**, *19*, 4030–4035. (c) McGrady, G. S.; Turner, J. F. C.; Ibberson, R. M.; Prager, M. *Organometallics* **2000**, *19*, 4398–4401. (d) Klosin, J.; Roof, G. R.; Chen, E. Y.-X.; Abboud, K. A. *Organometallics* **2000**, *19*, 4684–4686. (e) Yu, Z.; Wittbrodt, J. M.; Heeg, M. J.; Schlegel, H. B.; Winter, C. H. *J. Am. Chem. Soc.* **2000**, *122*, 9338–9339. (f) Chen, E. Y.-X.; Abboud, K. A. *Organometallics* **2000**, *19*, 5541–5543. (g) Vanka, K.; Chan, M. S. W.; Pye, C. C.; Ziegler, T. *Organometallics* **2000**, *19*, 1841–1849. (h) Chan, M. S. W.; Ziegler, T. *Organometallics* **2000**, *19*, 5182–5189. (i) Schrock, R. R.; Casado, A. L.; Goodman, J. T.; Liang, L.-C.; Bonitatebus, P. J., Jr.; Davis, W. M. *Organometallics* **2000**, *19*, 5325–5341. (j) Duncan, A. P.; Mullins, S. M.; Arnold, J.; Bergman, R. G. *Organometallics* **2001**, *20*, 1808–1819. (k) Schumann, H.; Keitsch, M. R.; Demtschuk, J.; Molander, G. A. *J. Organomet. Chem.* **1999**, *582*, 70–82. (l) Schaverien, C. J. *Organometallics* **1994**, *13*, 69–82. (m) Chen, E. Y.-X.; Marks, T. J. *Chem. Rev.* **2000**, *100*, 1391–1434. (n) Song, X.; Thornton-Pett, M.; Bochmann, M. *Organometallics* **1998**, *17*, 1004–1006. (o) Kleinhenz, S.; Seppelt, K. *Chem.–Eur. J.* **1999**, *5*, 3573–3580. (p) Kulzick, M. A.; Andersen, R. A.; Muettterties, E. L.; Day, V. W. *J. Organomet. Chem.* **1987**, *336*, 221–236. (q) Schwartz, D. J.; Ball, G. E.; Andersen, R. A. *J. Am. Chem. Soc.* **1995**, *117*, 6027–6040. (r) Shin, J. H.; Parkin, G. *Chem. Commun.* **1998**, 1273–1274. (s) Chan, M. C. W.; Cole, J. M.; Gibson, V. C.; Howard, J. A. K. *Chem. Commun.* **1997**, 2345–2346. (t) Bursten, B. E.; Cayton, R. H. *Organometallics* **1986**, *5*, 1051–1053. (u) Ozawa, F.; Park, J. W.; Mackenzie, P. B.; Schaefer, W. P.; Henling, L. M.; Grubbs, R. H. *J. Am. Chem. Soc.* **1989**, *111*, 1319–1327. (v) Dawkins, G. M.; Green, M.; Orpen, A. G.; Stone, F. G. A. *J. Chem. Soc., Chem. Commun.* **1982**, 41–43. (w) Calvert, R. B.; Shapley, J. R. *J. Am. Chem. Soc.* **1978**, *100*, 7726–7727. (x) Hamilton, D. H.; Shapley, J. R. *Organometallics* **2000**, *19*, 761–769. (y) Schultz, A. J.; Williams, J. M.; Calvert, R. B.; Shapley, J. R.; Stucky, G. D. *Inorg. Chem.* **1979**, *18*, 319–323. (z) Dutta, T. K.; Vites, J. C.; Jacobsen, G. B.; Fehlner, T. P. *Organometallics* **1987**, *6*, 842–847. (aa) Adams, R. D.; Horváth, I. T. *Prog. Inorg. Chem.* **1985**, *33*, 127–181.
- (3) Carboranes: (a) Grimes, R. N. *Carboranes*; Academic Press: New York, 1970. (b) Olah, G. A.; Wade, K.; Williams, R. E. *Electron Deficient Boron and Carbon Clusters*; John Wiley & Sons: New York, 1991. (c) Kabalka, G. W. *Current Topics in the Chemistry of Boron*; The Royal Society of Chemistry: Cambridge, 1994. (d) Siebert, W. *Advances in Boron Chemistry*; The Royal Society of Chemistry: Cambridge, 1997. (e) King, R. B. *Boron Chemistry at the Millennium*; Elsevier Science: Amsterdam, 1999. (f) Davidson, M.; Hughes, A. K.; Marder, T. B.; Wade, K. *Contemporary Boron Chemistry*; The Royal Society of Chemistry: Cambridge, 2000.
- (4) Metal cluster cage: Scherbaum, F.; Grohmann, A.; Müller, G.; Schmidbauer, H. *Angew. Chem., Int. Ed. Engl.* **1989**, *28*, 463–465.
- (5) (a) Musher, J. I. *Angew. Chem., Int. Ed. Engl.* **1969**, *8*, 54–68. (b) Akiba, K.-y. *Chemistry of Hypervalent Compounds*; Wiley-VCH: New York, 1999.
- (6) (a) Yamabe, S.; Yamabe, E.; Minato, T. *J. Chem. Soc., Perkin Trans. 2* **1983**, 1881–1884. (b) Ruggiero, G. D.; Williams, I. H. *J. Chem. Soc., Perkin Trans. 2* **2001**, 448–458. (c) Carroll, M. T.; Gordon, M. S.; Windus, T. L. *Inorg. Chem.* **1992**, *31*, 825–829. (d) Glukhovtsev, M. N.; Pross, A.; Radom, L. *J. Am. Chem. Soc.* **1995**, *117*, 2024–2032. (e) Hiraoaka, K.; Nasu, M.; Fujimaki, S.; Ignacio, E. W.; Yamabe, S. *Chem. Phys. Lett.* **1995**, *245*, 14–18. (f) Raghavachari, K.; Chandrasekhar, J.; Burnier, R. C. *J. Am. Chem. Soc.* **1984**, *106*, 3124–3128.
- (7) Dean, J. A. *Lange's Handbook of Chemistry*, 11th ed.; McGraw-Hill: New York, 1973; pp 3-119–3-123.

- (8) (a) Grotewold, J.; Lissi, E. A.; Villa, A. E. *J. Chem. Soc. A* **1966**, 1034–1037. (b) Grotewold, J.; Lissi, E. A.; Villa, A. E. *J. Chem. Soc. A* **1966**, 1038–1041.
- (9) Toyota, S.; Futawaka, T.; Ikeda, H.; Oki, M. *J. Chem. Soc., Chem. Commun.* **1995**, 2499–2500.
- (10) (a) Breslow, R.; Garratt, S.; Kaplan, L.; LaFollette, D. *J. Am. Chem. Soc.* **1968**, *90*, 4051–4055. (b) Breslow, R.; Kaplan, L.; LaFollette, D. *J. Am. Chem. Soc.* **1968**, *90*, 4056–4064.
- (11) (a) Basalay, R. J.; Martin, J. C. *J. Am. Chem. Soc.* **1973**, *95*, 2565–2571. (b) Martin, J. C.; Basalay, R. J. *J. Am. Chem. Soc.* **1973**, *95*, 2572–2578.

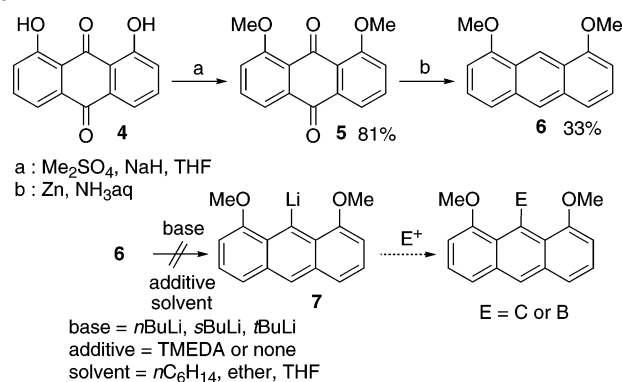
ment between the two sulfonium salts. Forbus and Martin claimed the synthesis and direct observation of pentacoordinate carbon compound using the 1,8-bis(*p*-methylphenylthio)anthracenyl ligand, where the carbocation attached at C-9 is contained in a benzene ring bearing two methoxy groups at 2',6'-positions.<sup>12</sup> The <sup>13</sup>C NMR chemical shift of the central carbon ( $\delta$  109 ppm; dication) was shifted to higher field from the reduced electronically neutral anthracene compound ( $\delta$  118 ppm). Although they carefully tried to prove the existence of pentacoordinate carbon compounds with NMR, which showed a symmetrical spectrum apparently reasonable as pentacoordinate species in solution, the compounds had not been characterized by X-ray analysis. In 1984, Lee and Martin reported direct observation of hypervalent penta- ( $\delta_B -20$  ppm) and hexacoordinate ( $\delta_B -123$  ppm) boron compounds with the use of <sup>11</sup>B NMR.<sup>13</sup> The latter <sup>11</sup>B NMR chemical shift was the highest value ever observed for any known boron compound with only first-row elements bonded to the central boron atom. Then, the Hojo group attempted to prepare a pentacoordinate carbon compound by stabilizing the carbocation attached at the C-1 of fluorene by coordination of the two methylthio groups at C-9.<sup>14</sup> However, in the solid state the two C<sup>+</sup>-S bond distances were different, with the shorter one (1.94 Å) close to that of a covalent C-S bond (1.81 Å), forming a sulfonium salt. Kudo detected CLi<sub>6</sub>, which was proposed by the Schleyer group,<sup>15</sup> by Knudsen-effusion mass spectrometry.<sup>16</sup> However, the details of the bonding nature of CLi<sub>5</sub> and CLi<sub>6</sub> have not yet been clarified.

Recently, we reported on the syntheses and X-ray structures of several carbon<sup>17a-e</sup> and boron<sup>17b-d</sup> compounds bearing a newly synthesized rigid tridentate anthracene ligand. However, there appeared comments by a chemist about the intrinsic nature of the hypervalent interaction between the central carbon and the two coordinating oxygen atoms.<sup>18</sup> Here we report on the details of our work, especially on the structures of the carbon and the corresponding boron compounds with anthracene ligands. The bonding nature between the central carbon (or boron) and the two coordinating atoms is elucidated and discussed based on the several X-ray structures with several different substituents, theoretical DFT calculations, and the accurate experimental X-ray electron-density distribution analysis. The structures and the bonding nature of newly synthesized pentacoordinate carbon compounds bearing a 2,6-bis(*p*-substituted phenyloxymethyl)-benzene ligand will be discussed in a separate paper.<sup>19</sup>



**Figure 2.** Ligand design for pentacoordinate carbon and boron compounds.

**Scheme 1.** Attempted *peri*-Lithiation of 1,8-Dimethoxyanthracene **6**



**Results and Discussion**

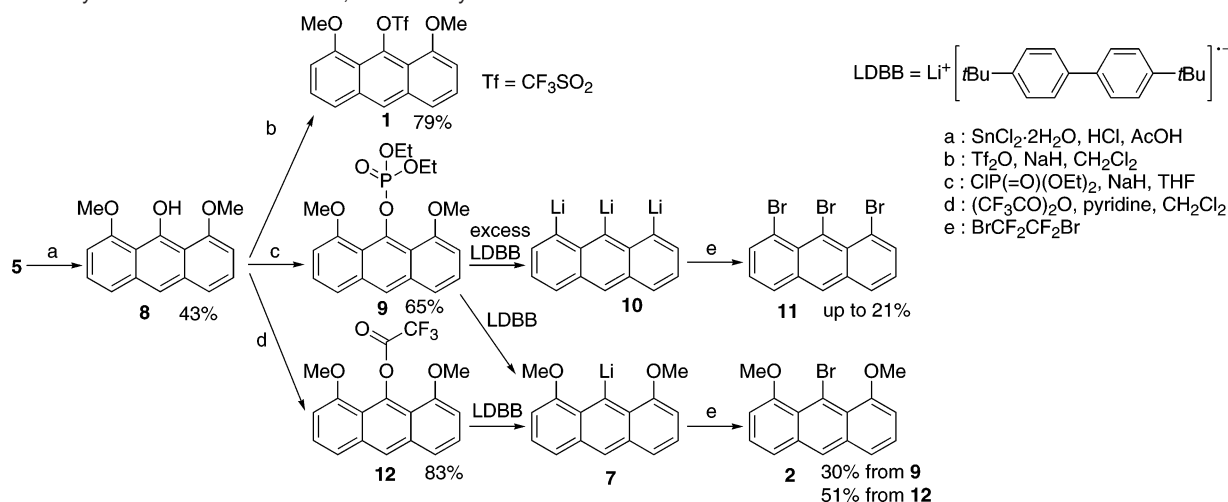
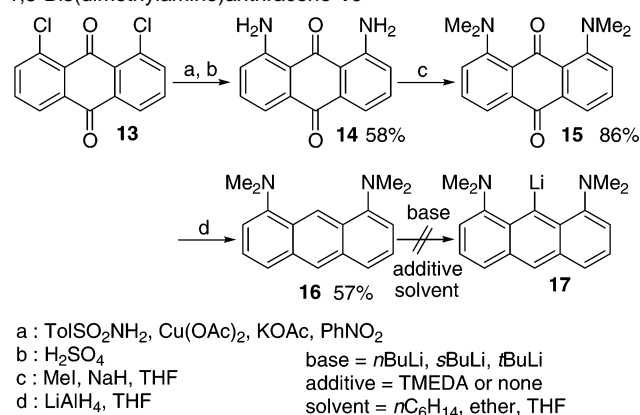
**Strategy for the Synthesis of Hypervalent Pentacoordinate Carbon (10-C-5) and Boron (10-B-5) Compounds.** To stabilize the pentacoordinate carbon (10-C-5) and boron (10-B-5) species, we used a rigid anthracene skeleton with donor groups D (Figure 2), and the ligand precursors **1–3** were synthesized (Figure 2).

**Syntheses of Ligand Precursors **1** and **2**.** A direct lithiation of the 9-position of 1,8-dimethoxyanthracene **6**,<sup>20a</sup> which was prepared from commercially available anthraquinone **4**, was examined under various conditions with various bases (*n*-BuLi, *s*-BuLi, *tert*-BuLi) in various solvents (*n*-hexane, diethyl ether, tetrahydrofuran) with or without the addition of *N,N,N',N'*-tetramethylethylenediamine (TMEDA). However, the desired lithiation at the 9-position to give **7** did not occur at all (Scheme 1). Therefore, 9-hydroxy anthracene **8**<sup>20b</sup> was converted to triflate **1** (Scheme 2), which was useful for the introduction of the carbon atom at the 9-position.<sup>17a</sup> Since **1** could not be used for the introduction of the boron atom, 9-bromoanthracene precursor **2** had to be synthesized.<sup>17b</sup>

1,8-Dimethoxy-9-bromoanthracene **2** was synthesized from **8** with a selective C–O bond cleavage reaction from **9** or **12** as a key step (Scheme 2). Initially, several reduction conditions were examined for phosphate **9**,<sup>17b</sup> with a couple of one-electron reducing reagents (K/NH<sub>3</sub>, lithium naphthalenide, etc.). The reduction of **9** under K/NH<sub>3</sub> (Birch reduction condition) gave 9-protonated product **6**, which should be generated by the reaction of the 9-potassium derivative with ammonia. To prevent the trapping of a proton, THF was chosen as an aprotic solvent, and the reduction of **9** was carried out with lithium naphthalenide followed by the reaction with BrCF<sub>2</sub>CF<sub>2</sub>Br. The reaction gave

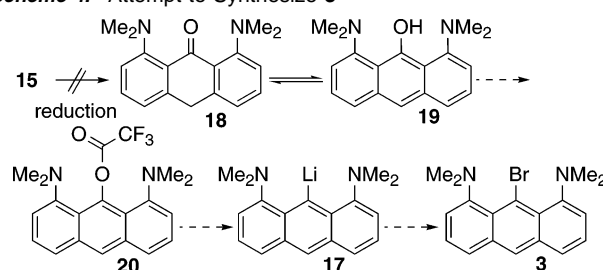
- (12) (a) Forbus, T. R., Jr.; Martin, J. C. *J. Am. Chem. Soc.*, **1979**, *101*, 5057–5059. (b) Forbus, T. R., Jr. Ph.D. Thesis, University of Illinois, 1981. (c) Forbus, T. R., Jr.; Martin, J. C. *Heteroat. Chem.* **1993**, *4*, 113–128. (d) Forbus, T. R., Jr.; Martin, J. C. *Heteroat. Chem.* **1993**, *4*, 129–136. (e) Forbus, T. R., Jr.; Kahl, J. L.; Martin, J. C. *Heteroat. Chem.* **1993**, *4*, 137–143. (f) Martin, J. C. *Science* **1983**, *221*, 509–514.
- (13) (a) Lee, D. Y.; Martin, J. C. *J. Am. Chem. Soc.* **1984**, *106*, 5745–5746. (b) Lee, D. Y., Ph.D. Thesis, University of Illinois, 1985.
- (14) Hojo, M.; Ichi, T.; Shibato, K. *J. Org. Chem.* **1985**, *50*, 1478–1482.
- (15) Schleyer, P. v. R.; Würthwein, E.-U.; Kaufmann, E.; Clark, T. *J. Am. Chem. Soc.* **1983**, *105*, 5930–5932.
- (16) Kudo, H. *Nature*, **1992**, *355*, 432–434.
- (17) (a) Akiba, K.-y.; Yamashita, M.; Yamamoto, Y.; Nagase, S. *J. Am. Chem. Soc.* **1999**, *121*, 10644–10645. (b) Yamashita, M.; Yamamoto, Y.; Akiba, K.-y.; Nagase, S. *Angew. Chem., Int. Ed.* **2000**, *39*, 4055–4058. (c) Yamashita, M.; Watanabe, K.; Yamamoto, Y.; Akiba, K.-y. *Chem. Lett.* **2001**, 1104–1105. (d) Yamashita, M.; Kamura, K.; Yamamoto, Y.; Akiba, K.-y. *Chem.-Eur. J.* **2002**, *8*, 2976–2979. (e) Yamashita, M.; Mita, Y.; Yamamoto, Y.; Akiba, K.-y. *Chem.-Eur. J.* **2003**, *9*, 3655–3659.
- (18) Levy, J. B. *Chem. Eng. News* **2000**, *78*, 13–14.
- (19) Akiba, K.-y.; Moriyama, Y.; Mizozoe, M.; Inohara, H.; Nishii, T.; Yamamoto, Y.; Minoura, M.; Hashizume, D.; Iwasaki, F.; Takagi, N.; Ishimura, K.; Nagase, S. *J. Am. Chem. Soc.* In press.

- (20) (a) Cameron, D. W.; Schütz, P. E. *J. Chem. Soc. C* **1967**, 2121–2125. (b) Prinz, H.; Burgemeister, T.; Wiegreb, W.; Müller, K. *J. Org. Chem.* **1996**, *61*, 2857–2860.

**Scheme 2.** Syntheses of 9-Substituted 1,8-Dimethoxyanthracenes **1** and **2****Scheme 3.** Attempted *peri*-Lithiation of 1,8-Bis(dimethylamino)anthracene **16**

a complex mixture including the starting material **9** and a very small amount of the desired product **2**. Substitution of the one-electron reducing reagent to lithium 4,4'-di-*tert*-butylbiphenylide (LDBB), which has a higher reduction potential, improved the yield of **2** up to 30%. When an excess amount of LDBB was used, an undesired product 1,8,9-tribromoanthracene **11** (ca. 20%) was obtained instead of **2**. The formation of **11** should be explained via 1,8,9-trilithioanthracene **10**, which was reacted with  $\text{BrCF}_2\text{CF}_2\text{Br}$  to form **11**. Finally, a more efficient route via a trifluoroacetoxy intermediate **12** was found, and the total yield of **2** was improved to 51% from **12**.

**Synthesis of Ligand Precursor 3.** Initially, a direct lithiation of the 9-position of 1,8-bis(dimethylamino)anthracene **16**,<sup>23</sup> which was prepared from **13**, **14**,<sup>21</sup> and **15**,<sup>22</sup> was examined (Scheme 3), but the desired lithiation of the 9-position to **17** did not take place at all. In addition, a strategy to use 1,8-bis(dimethylamino)anthrone **18** or tautomerized 1,8-bis(dimethylamino)-9-hydroxyanthracene **19** as a synthetic intermediate (Scheme 4), which is based on the previous synthesis of 1,8-dimethoxy-9-bromoanthracene **2**, did not work because the reduction of 1,8-bis(dimethylamino)anthraquinone **15** to the corresponding anthrone **18** was not successful.

**Scheme 4.** Attempt to Synthesize **3**

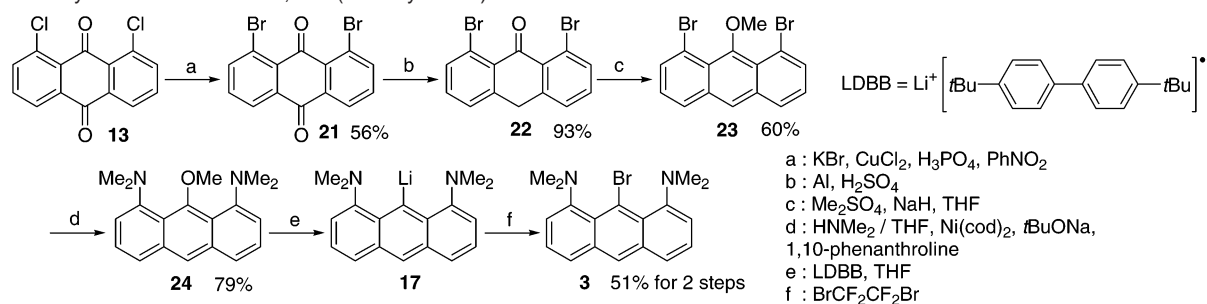
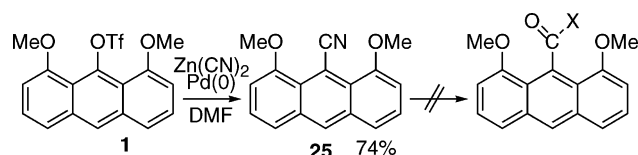
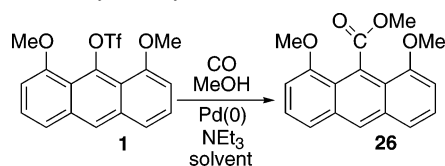
Finally, **3** could be prepared as illustrated in Scheme 5.<sup>17d</sup> Bromide substitution<sup>24</sup> of commercially available dichloroanthraquinone **13** followed by reduction<sup>25</sup> afforded dibromoanthrone (**22**) in 52% yield from **13**. Deprotonation of **22** followed by methylation gave 1,8-dibromo-9-methoxyanthracene (**23**) in 60% yield. The Pd(0) mediated coupling reaction of **23** with various nucleophiles ( $\text{Bu}_3\text{SnNMe}_2$ ,  $\text{Me}_3\text{SnNMe}_2$ ,  $\text{LiNMe}_2$ , and  $\text{HNMe}_2$ ) did not give the expected bis-dimethylaminated compound (**24**); instead only a mono-dimethylaminated product was obtained in most cases, and the reduction of the C–Br bonds took place in some cases. However, dibromoanthracene **23** could be converted to 1,8-bis(dimethylamino)-9-methoxyanthracene **24** in 79% yield by heating a  $\text{HNMe}_2$ –THF solution of **23** up to 150 °C in a pressure-resistant vessel with a Ni(0) catalyst, which is a modified Buchwald's method.<sup>26</sup> LDBB (lithium di-*tert*-butylbiphenylide) reduction of the methoxy group at the 9-position of the anthracene skeleton worked well for **24** to afford the novel anthracene ligand precursor **3** in 51% yield after reaction with  $\text{BrCF}_2\text{CF}_2\text{Br}$ .

**Pentacoordinate Hypervalent Carbon Compound (10-C-5). A. Introduction of a Carbon Atom to the 9-Position of Anthracene.** Initially, the Pd-mediated coupling reaction of ligand **1** was examined in order to introduce a carbon substituent (Scheme 6). Nitrile **25** was obtained in 74% yield by the reaction of **1** with  $\text{Zn}(\text{CN})_2$  in DMF in the presence of a Pd(0) catalyst.<sup>27</sup>

However, the conversion from **25** was very sluggish; only ca. 5% of the corresponding ethyl ester could be obtained after

(21) House, O. H.; Koepsell, D. G.; Campbell, W. J. *J. Org. Chem.* **1972**, *37*, 1003–1011.  
 (22) Lord, W. M.; Peters, A. T. *J. Chem. Soc. C* **1968**, *7*, 783–785.  
 (23) Haenel, M. W.; Oevers, S.; Bruckmann, J.; Kuhnigk, J.; Krüger, C. *Synlett* **1998**, 301–303.

(24) Benites, M. del R.; Fronczek, F. R.; Hammer, R. P.; Maverick, A. W. *Inorg. Chem.* **1997**, *36*, 5826–5831.  
 (25) Biehl, R.; Hinrichs, K.; Kurreck, H.; Lubitz, W. Mennenga, U.; Roth, K. *J. Am. Chem. Soc.* **1977**, *99*, 4278–4286.  
 (26) Wolfe, J. P.; Buchwald, S. L. *J. Am. Chem. Soc.* **1997**, *119*, 6054–6058.  
 (27) Kubota, H.; Rice, K. C. *Tetrahedron Lett.* **1998**, *39*, 2907–2910.

**Scheme 5.** Synthesis of 9-Bromo-1,8-bis(dimethylamino)anthracence **3****Scheme 6.** Introduction of a Nitrile Group to the 9-Position of the Anthracene Skeleton**Scheme 7.** Methoxycarbonylation of **1**

treatment with excess amounts of CF<sub>3</sub>SO<sub>3</sub>H, H<sub>2</sub>O, and EtOH at 80 °C for 3.5 days. Strong hydride reagents (super-H, DIBAL-H) did not work either.

Since the conversion of **25** was not quite successful, the direct methoxycarbonylation of **1** was examined (Scheme 7, Table 1). Based on the method in the literature,<sup>28</sup> **1** was treated with MeOH, Pd(II) catalyst, and NEt<sub>3</sub> in DMSO under CO atmosphere; however, the starting material **1** was recovered (entry 1). Since the poor results may be due to the difficulty of the generation of active Pd(0) species from Pd(II) species without a reductant, Pd(PPh<sub>3</sub>)<sub>4</sub> was used instead of Pd(II). In the presence of Pd(PPh<sub>3</sub>)<sub>4</sub>, the use of DMF as a solvent did not work (entry 2). However, the combination of DMSO as a solvent and Pd(PPh<sub>3</sub>)<sub>4</sub> as catalyst afforded the desired product **26** in 37% yield (entry 3). A longer reaction time raised the yield of **26** slightly better (entry 4, 52%).

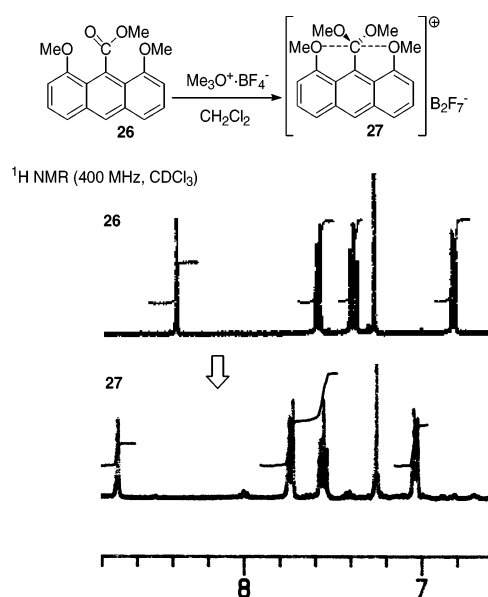
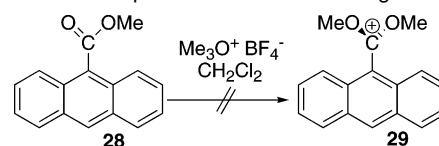
**B. Generation and Characterization of Hypervalent Pentacoordinate Carbon Compound 27.** To generate carbocation **27**, ester derivative **26** was treated with an excess amount of Meerwein reagent (Me<sub>3</sub>O<sup>+</sup>BF<sub>4</sub><sup>-</sup>)<sup>29</sup> in refluxing CH<sub>2</sub>Cl<sub>2</sub> for 20 h (Figure 3). After filtration of excess Me<sub>3</sub>O<sup>+</sup>BF<sub>4</sub><sup>-</sup> and removal of the solvent, **27** was obtained as a yellow-green solid. In the <sup>1</sup>H NMR of **27**, all of the aromatic peaks showed the symmetric structure of anthracene skeleton just like **26** and shifted to lower fields with the retention of four kinds of peaks (two kinds of doublets, a triplet and a singlet).

In the use of 9-methoxycarbonylanthracene **28** without two OMe groups at the 1,8-position of the anthracene skeleton, the generation of the corresponding carbocation was not observed in <sup>1</sup>H NMR (Scheme 8). The lack of reactivity in **28** may result from a lack of hypervalent bonding interaction between the

**Table 1.** Conditions for Methoxycarbonylation of **1**

run	catalyst	solvent	temp, °C	time, h	result
1	Pd(OAc) <sub>2</sub> /dppf <sup>a</sup>	DMSO	70	2	no reaction
2	Pd(PPh <sub>3</sub> ) <sub>4</sub>	DMF	130	2	no reaction
3	Pd(PPh <sub>3</sub> ) <sub>4</sub>	DMSO	70	2	<b>26</b> (37%)
4	Pd(PPh <sub>3</sub> ) <sub>4</sub>	DMSO	70	8	<b>26</b> (52%)

<sup>a</sup> dppf: diphenylphosphiniferrocene.

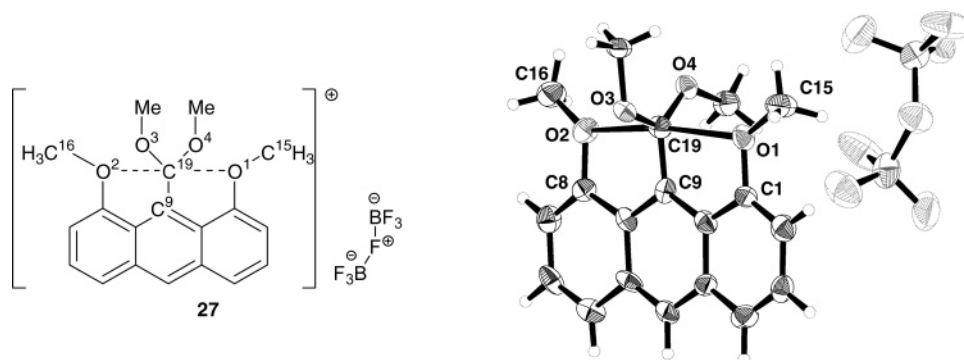
**Figure 3.** Generation of pentacoordinate hypervalent carbon compound **27**.**Scheme 8.** Attempted Methylation of the Methoxycarbonyl Group without Two OMe Groups on the Anthracene Ring

carbocation center and the lone pairs of the OMe groups. This fact indirectly supported the existence of a hypervalent stabilizing interaction between the central carbon and the two OMe groups in **27**.

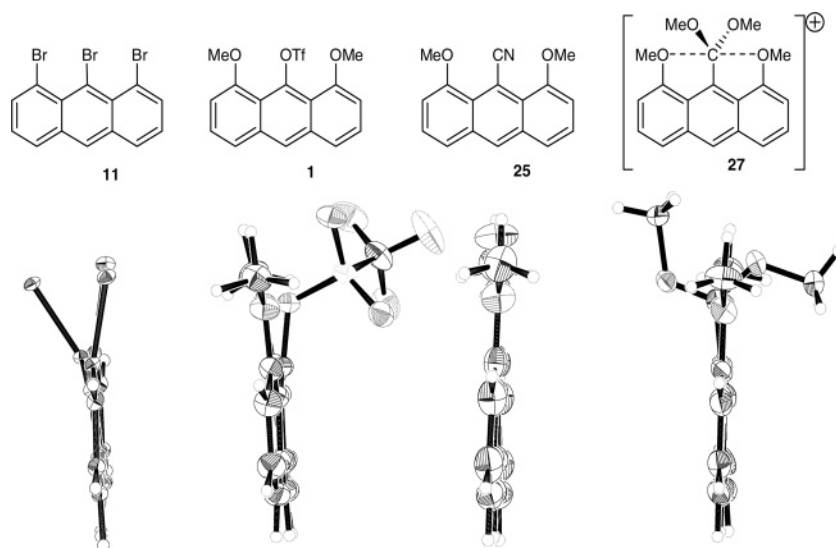
To determine the <sup>13</sup>C NMR chemical shift of the central carbon of **27** clearly, <sup>13</sup>C-**26** and <sup>13</sup>C-**27** were synthesized. Esterification of **1** proceeded under <sup>13</sup>C-enriched CO atmosphere to give <sup>13</sup>C-**26**. The ester was similarly methylated by Me<sub>3</sub>O<sup>+</sup>BF<sub>4</sub><sup>-</sup> to give <sup>13</sup>C-**27**. In the <sup>13</sup>C NMR spectra, the chemical shift of the central carbon shifted from δ 172.30 (<sup>13</sup>C-**26**) to δ 192.58 (<sup>13</sup>C-**27**) ppm. The difference in the chemical shifts (Δδ = 20.28) was comparable to the difference (Δδ = 21.3) from

(28) Dolle, R. E.; Schmidt, S. J.; Kruse, L. I. *J. Chem. Soc., Chem. Commun.* **1987**, 904–905.

(29) Meerwein, H. *Methoden Org. Chim.* **1965**, 6/3, 325–365.



**Figure 4.** ORTEP drawing of **27** (30% thermal ellipsoid). Selected bond distances (Å) and angles (deg): C<sup>19</sup>–O<sup>1</sup> 2.43(1), C<sup>19</sup>–O<sup>2</sup> 2.45(1), C<sup>19</sup>–O<sup>3</sup> 1.26(1), C<sup>19</sup>–O<sup>4</sup> 1.30(1), C<sup>19</sup>–C<sup>9</sup> 1.48(1), O<sup>1</sup>–C<sup>19</sup>–O<sup>2</sup> 168.7(5), O<sup>1</sup>–C<sup>19</sup>–O<sup>3</sup> 95.7(7), O<sup>1</sup>–C<sup>19</sup>–O<sup>4</sup> 90.5(6), O<sup>1</sup>–C<sup>19</sup>–C<sup>9</sup> 85.4(7), O<sup>2</sup>–C<sup>19</sup>–O<sup>3</sup> 94.6(7), O<sup>2</sup>–C<sup>19</sup>–O<sup>4</sup> 88.8(6), O<sup>2</sup>–C<sup>19</sup>–C<sup>9</sup> 85.8(6), O<sup>3</sup>–C<sup>19</sup>–O<sup>4</sup> 117.9(9), O<sup>3</sup>–C<sup>19</sup>–C<sup>9</sup> 116.3(8), O<sup>4</sup>–C<sup>19</sup>–C<sup>9</sup> 125.8(9).



**Figure 5.** Comparison of side views of **11**, **1**, **25**, and **27**.

methyl formate ( $\delta$  171.52)<sup>30</sup> to dimethoxymethyl cation ( $\delta$  192.8).<sup>31</sup>

From the CDCl<sub>3</sub> solution of **27**, single crystals suitable for X-ray analysis were obtained, and the X-ray structure is shown in Figure 4. The counteranion B<sub>2</sub>F<sub>7</sub><sup>−</sup> is unexpected, but it is well separated from the cationic part. The structure clearly shows the symmetrical nature of the compound. The sum of the angles (O<sup>3</sup>–C<sup>19</sup>–C<sup>9</sup>, O<sup>4</sup>–C<sup>19</sup>–C<sup>9</sup>, and O<sup>3</sup>–C<sup>19</sup>–O<sup>4</sup>) around the central carbon is 360.0°, indicating that the carbon is planar with sp<sup>2</sup> hybridization. The angles around the oxygen atoms of the methoxy group at the 1,8-positions of anthracene are 119.2(9)° (C<sup>1</sup>–O<sup>1</sup>–C<sup>15</sup>) and 120.3(9)° (C<sup>8</sup>–O<sup>2</sup>–C<sup>16</sup>), showing that both oxygen atoms have sp<sup>2</sup> hybridization. Since the carbon atoms of the methoxy groups at the 1,8-positions are in the plane of the anthracene, one of the lone pairs of each oxygen atom should be directed toward the empty p-orbital of the central carbocation attached at the 9-position and the other should be parallel to  $\pi$ -electrons of the anthracene. Therefore, the geometry around the central carbon atom is TBP, which is only slightly distorted. The two C–O distances are almost identical [2.43(1) and 2.45(1) Å], which is significantly longer than that of a covalent C–O bond (1.43 Å)<sup>7</sup> but shorter than the corresponding apical C–O

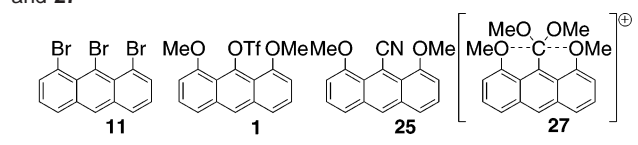
bond (2.64 Å) in the transition state of [H<sub>2</sub>O–C(CH<sub>3</sub>)<sub>3</sub>–OH<sub>2</sub>]<sup>+</sup>.<sup>6a</sup> The ratio of the observed C–O apical length of **27** to the sum of the covalent radius was 1.71. The elongation of the C–O bond is comparable to [H<sub>2</sub>O–C(CH<sub>3</sub>)<sub>3</sub>–OH<sub>2</sub>]<sup>+</sup> (the ratio of the apical C–O bond to the sum of the covalent radius is 1.84).<sup>6a</sup>

**C. Elucidation of the Weak C–O Interaction in 27.** To elucidate the property and the degree of interaction between the central carbon atom and the two oxygen atoms in **27**, the side views of the crystal structures and selected distances of **11**, **1**, and **25** are shown in Figure 5 together with **27**. In the structure of tribromo derivative **11**, the three bromine atoms are placed out of plane of the anthracene skeleton in order to avoid large steric repulsion. In the structure of **1**, three oxygen atoms are slightly distorted from the anthracene plane, probably due to the lone-pair repulsion among the three oxygens.

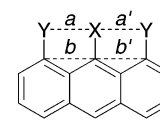
In the case of **25** and the cation **27**, the atoms attached to the 1, 8, and 9 positions are almost perfectly in the plane of the anthracene, indicating that the interaction between the central carbon atom and the two oxygen atoms is not repulsive. The comparison of the distances between the atom attached to the 9-position of the anthracene and the atoms on the 1,8-positions is also worthy of note (Table 2). In the cases of **11** and **1**, the averaged distances of *a* and *a'* (3.2698(6) Å in **11**, 2.572(2) Å in **1**) are longer than those of *b* and *b'* (2.566(6) Å in **11**, 2.550-

(30) SDBSWeb: <http://www.aist.go.jp/RIODB/SDBS/menu-j.html>.

(31) Olah, G. A.; Hartz, N.; Rasul, G.; Burrichter, A.; Prakash, G. K. S. *J. Am. Chem. Soc.* **1995**, *117*, 6421–6427.

**Table 2.** Comparison of Distances of  $a$  ( $a'$ ) and  $b$  ( $b'$ ) of **11**, **1**, **25**, and **27**


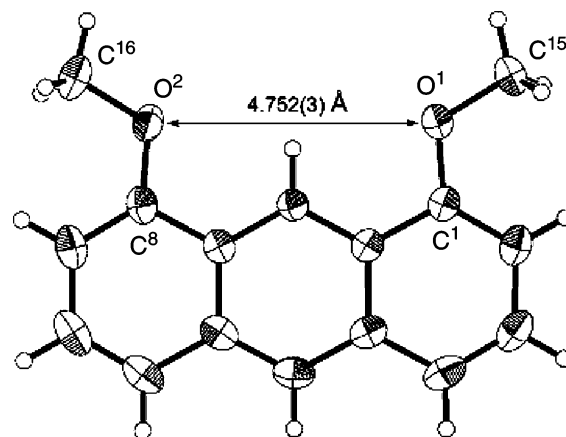
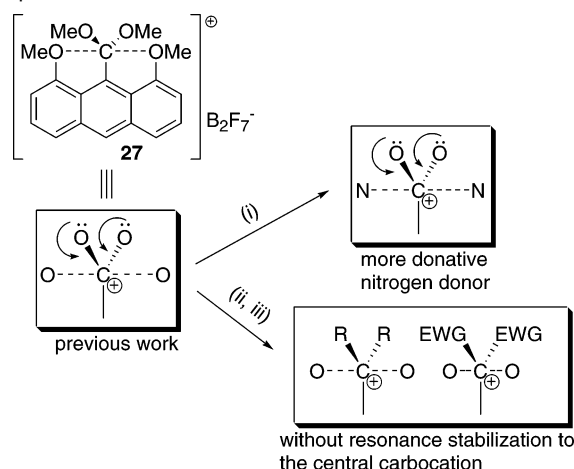
	<b>11</b>	<b>1</b>	<b>25</b>	<b>27</b>
$a$	3.2658(6)	2.572(2)	2.530(3)	2.45(1)
$a'$	3.2738(6)	2.571(2)	2.531(3)	2.43(1)
$b$	2.564(6)	2.554(3)	2.538(6)	2.49(2)
$b'$	2.567(6)	2.545(3)	2.542(4)	2.52(2)



(3) Å in **1**), while, in **25**, the averaged distance of  $a$  and  $a'$  (2.531(3) Å) is comparable with that of  $b$  and  $b'$  (2.540(5) Å). In contrast, in **27**, the averaged distance of  $a$  and  $a'$  (2.44(1) Å) is clearly shorter than that of  $b$  and  $b'$  (2.51(2) Å). Therefore, it can be concluded that the interaction between the central carbon atom and the two oxygen atoms in **27** should be clearly attractive.

To elucidate the nature of the interaction between the central carbon atom and the two oxygen atoms at the 1,8-positions of anthracene skeleton, the geometry of **27** was fully optimized with hybrid density functional theory (DFT) at the B3PW91/6-31G(d) level using the Gaussian 98 program.<sup>32</sup> The structural optimization afforded the symmetrical  $C_s$  structure of **27** as the energy minimum. The two C–O distances are identical (2.472 Å) and slightly longer than the experimental distances (2.43(1) and 2.45(1) Å). It should be noted that the bond paths are found between the central carbon atom and the two oxygen atoms, clearly showing that these atoms are bonded.<sup>33</sup> The bond is weak and ionic based on the small  $\rho(\mathbf{r})$  value of 0.022  $e/a_0^3$  and the small positive  $\nabla^2\rho(\mathbf{r})$  value of 0.080  $e/a_0^5$  at the bond critical points. These values are consistent with those of axial C–H bonds in  $\text{CH}_5^-$  ( $\rho(\mathbf{r})$ : 0.067  $e/a_0^3$ ,  $\nabla^2\rho(\mathbf{r})$ : 0.009  $e/a_0^5$ ).<sup>6c</sup> A large value (0.219) of the ellipticity of the C–O bond reflects the electron donation to the central carbocation from the two lone pairs of the oxygen atoms of the methoxy groups at the 1,8-positions within the anthracene plane. In conclusion, the anthracene carbocation **27** is the first fully characterized hypervalent pentacoordinate 10-C-5 compound for a model of the transition state of the  $S_N2$  reaction.

Recently, a comment appeared in *C&E News*, discussing the weak interaction between the central carbon atom and two oxygen atoms at 1,8-positions of anthracene skeleton in **27**.<sup>18</sup> It stated that “The two methoxy groups at the 1 and 8 positions of **27** lean toward one another in the analogous conformation

**Figure 6.** ORTEP drawing of **6** (30% thermal ellipsoid). Selected interatomic distances (Å) and angles (deg): C<sup>1</sup>–O<sup>1</sup> 1.366(2), C<sup>8</sup>–O<sup>2</sup> 1.359(2), C<sup>15</sup>–O<sup>1</sup> 1.423(2), C<sup>16</sup>–O<sup>2</sup> 1.425(2), O<sup>1</sup>–O<sup>2</sup> 4.752(3), C<sup>1</sup>–O<sup>1</sup>–C<sup>15</sup> 117.62(16), C<sup>8</sup>–O<sup>2</sup>–C<sup>16</sup> 117.77(17).**Scheme 9.** Strategy for the Derivatization of Hypervalent Carbon Compounds

of 1,8-dimethoxyanthracene, without a central positive carbon”. Therefore, we examined the X-ray structure of 1,8-dimethoxyanthracene **6** (Figure 6), which showed a relatively shorter O<sup>1</sup>–O<sup>2</sup> distance [4.752(3) Å] than the sum of two apical C–O distances of **27** (4.88 Å) as the commentator indicated. Therefore, we started further investigation to obtain the hypervalent pentacoordinate carbon (or boron) compounds bearing stronger apical C–O (or B–O) interaction.

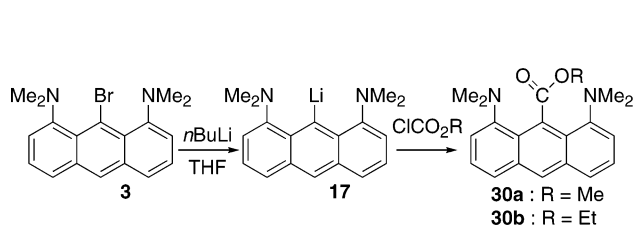
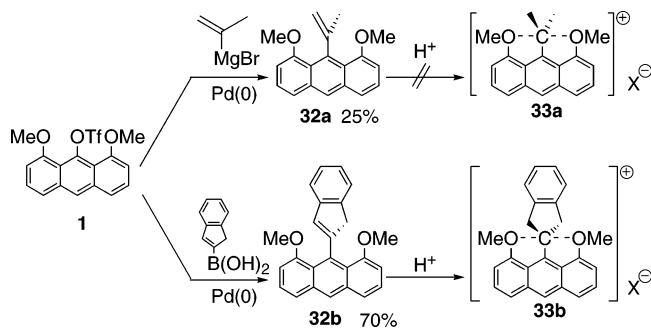
**D. Attempt to Synthesize Other Hypervalent Pentacoordinate Carbon Compounds.** The strategy for derivatization of hypervalent pentacoordinate carbon compounds with stronger apical C–O interaction is illustrated in Scheme 9. To strengthen the apical bond, three types of derivatizations were examined. (i) Apical oxygen atoms were replaced by nitrogen atoms to strengthen the electron-donating ability of the donor. (ii, iii) Substituents on the  $sp^2$  plane of the carbocation were replaced by alkyl or perfluoroalkyl groups to reduce the electron density on the central carbocation. However, the attempt to obtain the X-ray structures has not been successful until now. The synthesis and results are briefly shown below.

The synthesis of the carbocation species bearing the nitrogen donor ligand and its precursor is illustrated in Scheme 10. Halogen lithium exchange reaction of **3** with  $n$ -BuLi generated the corresponding lithium derivative **17** quantitatively, followed by esterification with  $\text{ClCO}_2\text{R}$  (R = Me, Et) to give the

(32) Frisch, M. J.; Trucks, G. W.; Schlegel, H. B.; Scuseria, G. E.; Robb, M. A.; Cheeseman, J. R.; Zakrzewski, V. G.; Montgomery, J. A.; Stratmann, R. E., Jr.; Burant, J. C.; Dapprich, S.; Millam, J. M.; Daniel, A. D.; Kudin, S. K. N.; Strain, M. C.; Farkas, O.; Tomasi, J.; Barone, V.; Cossi, M.; Cammi, R.; Mennucci, B.; Pomelli, C.; Adamo, C.; Clifford, S.; Ochterski, J.; Petersson, G. A.; Ayala, P. Y.; Cui, Q.; Morokuma, K.; Malick, D. K.; Rabuck, A. D.; Raghavachari, K.; Foresman, J. B.; Cioslowski, J.; Ortiz, J. V.; Stefanov, B. B.; Liu, G.; Liashenko, A.; Piskorz, P.; Komaromi, I.; Gomperts, R.; Martin, R. L.; Fox, D. J.; Keith, T.; Al-Laham, M. A.; Peng, C. Y.; Nanayakkara, A.; Gonzalez, C.; Challacombe, M.; Gill, P. M. W.; Johnson, B.; Chen, W.; Wong, M. W.; Andres, J. L.; Gonzalez, C.; Head-Gordon, M.; Replogle, E. S.; Pople, J. A. *Gaussian 98*, revision A.5; Gaussian, Inc.: Pittsburgh, PA, 1998.

(33) (a) Bader, R. F. W. *Atoms in Molecules – A Quantum Theory*; Oxford University Press: Oxford, 1990. (b) Bader, R. F. W. *Chem. Rev.* **1991**, *91*, 893–926. (c) Bader, R. F. W.; Slee, T. S.; Cremer, D.; Kraka, E. *J. Am. Chem. Soc.* **1983**, *105*, 5061–5068. (d) Bader, R. F. W. *J. Phys. Chem. A* **1998**, *102*, 7314–7323.



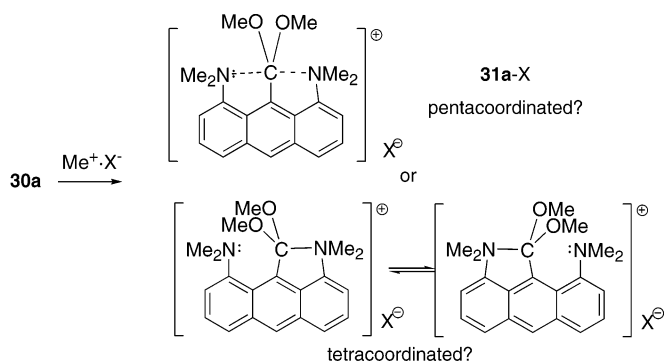
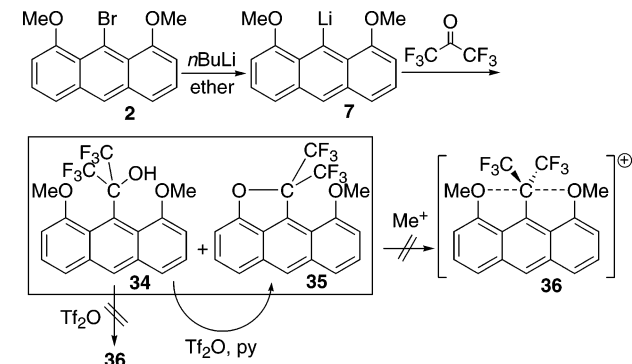
**Scheme 10.** Methoxycarbonylation of **3** and Methylation of **30a****Scheme 11.** Introduction of Olefins to 9-Position of Anthracene Skeleton

precursor **30a** (R = Me;  $\delta$  NMe<sub>2</sub> 2.67 (s, 6H) and 2.73 (s, 6H),  $\delta$  OMe 3.97 (s, 3H)) and **30b** (R = Et). In the generation of **31a-TfO<sup>-</sup>** or **31b-BF<sub>4</sub><sup>-</sup>** from **30a** or **30b** with MeOTf or Et<sub>3</sub>O<sup>+</sup>BF<sub>4</sub><sup>-</sup>, most of the product precipitated in a flask as an orange solid. The <sup>1</sup>H NMR spectrum of **31a-TfO<sup>-</sup>** could be measured in CD<sub>2</sub>Cl<sub>2</sub>, showing the lower-field-shifted symmetrical anthracene and NMe<sub>2</sub> pattern (lower; aliphatic, 12H singlet of NMe<sub>2</sub> ( $\delta$  2.96), 6H singlet of OMe ( $\delta$  3.94); aromatic, two doublets, a triplet and a singlet), which was similar to that of **27** (Figure 4). A variety of attempts to obtain a single crystal of **31a-X<sup>-</sup>** suitable for X-ray analysis were not successful even when the counteranion was exchanged to ClO<sub>4</sub><sup>-</sup> or B(C<sub>6</sub>F<sub>5</sub>)<sub>4</sub><sup>-</sup>.

Syntheses of the carbocations **33a** and **33b** bearing alkyl groups and their precursors are illustrated in Scheme 11. Ligand precursor **1** was reacted with metal-olefin reagents in the presence of a Pd(0) catalyst<sup>34,35</sup> to give the corresponding olefin products **32a** and **32b**. The double bond of **32a** and **32b** reacted with a proton to generate dialkyl carbocation **33a** and **33b**, respectively.

In the case of **33a**, the <sup>1</sup>H NMR spectrum showed a complicated pattern. On the other hand, the <sup>1</sup>H NMR spectrum of **33b** in the aromatic region showed the lower-field-shifted symmetrical anthracene pattern similar to that of **27** in addition to the identical CH<sub>2</sub> ( $\delta$  4.32) bonded to the central carbon. Unfortunately, any single crystal suitable for X-ray analysis could not be obtained for **33b**.

The attempted synthesis of the carbocation **36** bearing two trifluoromethyl groups is illustrated in Scheme 12. Lithium derivative **7** was reacted with gaseous hexafluoroacetone to give

**Scheme 12.** Introduction of a Carbon Atom Bearing Two Trifluoromethyl Groups to the Anthracene Skeleton

the alcohol **34** or cyclized demethylation compound **35**. The treatment of **34** with Tf<sub>2</sub>O gave cyclized demethylation compound **35** instead of carbocation derivative **36**. The attempted methylation of the oxygen of **35** to give desired carbocation **36** was not successful.

To obtain anionic hypervalent pentacoordinate carbon compound **38**, further demethylation of **35** was attempted (Scheme 13) with several reagents such as BBr<sub>3</sub>,<sup>36</sup> Me<sub>3</sub>SiI,<sup>37</sup> and HBr/Br<sup>-</sup>,<sup>38</sup> at low or high temperatures, but it gave no desired demethylated product **37** (Scheme 13). On the other hand, alkyllithium reacted with **35** to give unexpected products **39** and **40**.

To synthesize anionic hypervalent pentacoordinate carbon compound **38**, we designed a novel ligand precursor **45** bearing two deprotectable methoxymethyl groups as a trianion equivalent. Complete synthesis of a new ligand precursor **45** was already reported and is illustrated in Scheme 14.<sup>17e</sup> Synthesis of **45** was achieved with stepwise oxygenation with the oxaziridine reagent<sup>39</sup> and gaseous O<sub>2</sub>. Although **45** is not quite stable to chromatographic treatment (SiO<sub>2</sub>) or prolonged standing at room temperature, **45** could be purified by recycle HPLC.

After quantitative regeneration of lithium derivative **44** by the reaction of **45** with 1 equiv of *n*-BuLi in ether, **44** was reacted with gaseous hexafluoroacetone to give the alcohol derivative **46** together with cyclized product **47**. Cyclized product **47** was easily deprotected with HCl/THF at rt to give the precursor **37**. Compound **37** was deprotonated with KH in

(34) (a) Hayashi, T.; Niizuma, S.; Kamikawa, T.; Suzuki, N.; Uozumi, Y. *J. Am. Chem. Soc.* **1995**, *117*, 9101–9102. (b) Kamikawa, T.; Hayashi, T. *Synlett* **1997**, 163–164.

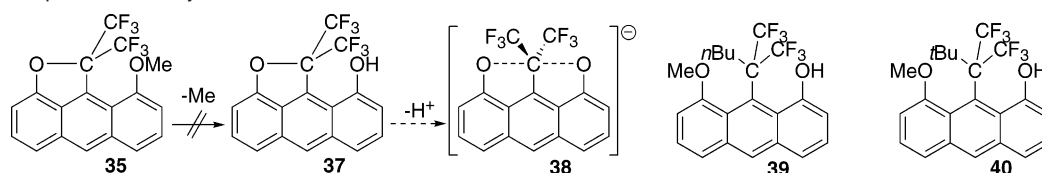
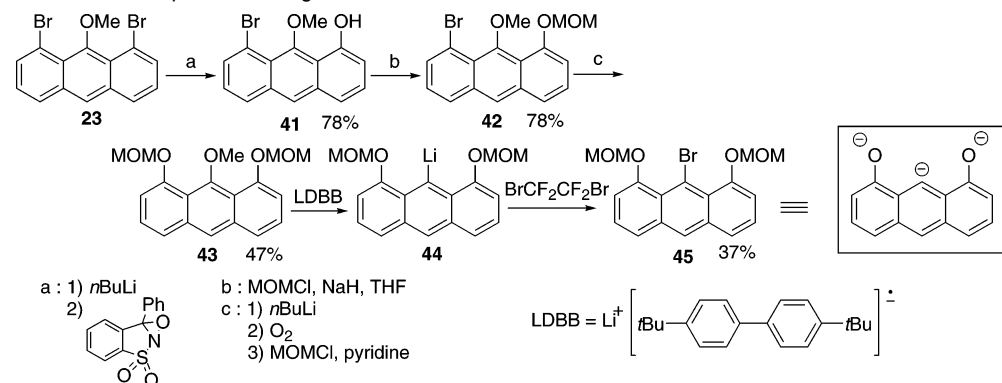
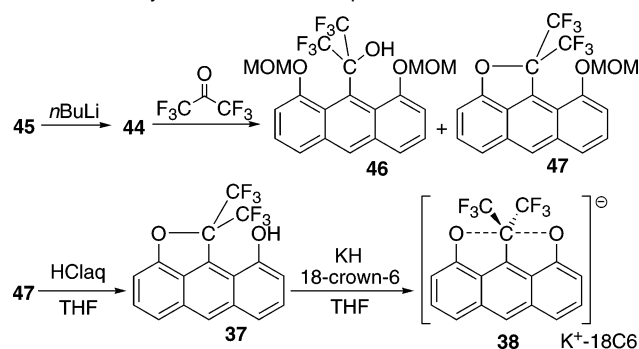
(35) (a) Ewen, I. M.; Rönnqvist, M.; Ahlberg, P. *J. Am. Chem. Soc.* **1993**, *115*, 3989–3996. (b) Shieh, W. C.; Carlson, J. A. *J. Org. Chem.* **1992**, *57*, 379–381. (c) Miyaura, N.; Suzuki, A. *Chem. Rev.* **1995**, *95*, 2457–2483.

(36) McOmie, J. F. W.; West, D. E. *Org. Synth. Collect. Vol.* **1973**, 412–414.

(37) Jung, M. E.; Lyster, M. A. *J. Org. Chem.* **1977**, *42*, 3761–3764.

(38) Hwang, K.; Park, S. *Synth. Commun.* **1993**, *23*, 2845–2849.

(39) Davis, F. A.; Towson, J. C.; Vashi, D. B.; ThimmaReddy, R.; McCauley, J. P., Jr.; Harakal, M. E.; Gosciniak, D. J. *J. Org. Chem.* **1990**, *55*, 1254–1261.

**Scheme 13.** Attempts for Demethylation of **35****Scheme 14.** Synthesis of New Deprotectable Ligand Precursor **45****Scheme 15.** Synthesis of Anionic Species **38**

the presence of 18-crown-6 to generate the desired anion species **38** (Scheme 15).

Single crystals of **38**, which slowly decomposed in air, suitable for X-ray analysis were obtained from THF–*n*-hexane solution under nitrogen atmosphere at room temperature. The ORTEP drawing of **38** is shown in Figure 7. The shorter O–C bond (O<sup>1</sup>–C<sup>15</sup>) length is 1.470(5) Å, and the longer O–C (O<sup>2</sup>–C<sup>15</sup>) length is 2.991(5) Å. Although the former is nearly equal to the sum (1.44 Å)<sup>7</sup> of the covalent radii of the carbon and oxygen atoms, the latter is shorter than that of the van der Waals radius (3.25 Å).<sup>7</sup> The potassium atom surrounded by a crown ether interacted with the phenoxide oxygen atom [O<sup>2</sup>–K<sup>1</sup>, 2.570(3) Å] in the solid state. An indicator, %TBPc,<sup>40</sup> for evaluation of the TBP character, showed that our compound **38** had low TBP character (27%) similar to pentacoordinate germanium compound **48** (Figure 8, 30%)<sup>39</sup> bearing a weak coordination. The structure of the carbon atom should be regarded to be common tetracoordinate carbon or pentacoordinate carbon bearing a very weak coordination. Although the bidentate ligand and electron-withdrawing group could lead a geometry around the germanium atom to have significant TBP character (87% from 30%) and weaken the interaction [O–K lengths; from 2.61–(1) Å to 2.881(6) Å] between an oxygen atom and a potassium atom surrounded by crown ether from **48** to **49** in the case of

hypervalent germanium compounds (Figure 8),<sup>41</sup> the tridentate ligand and two electron-withdrawing trifluoromethyl groups could not sufficiently affect a change in the structure of our carbon compound **38** from tetrahedral to TBP. This difference between our carbon compound **38** and germanium compounds **48** and **49** is probably due to the high electronegativity of the carbon atom, which could not sufficiently reduce the electron density on the central carbon atom to stabilize the hypervalent state of the carbon compounds. In this case, even the two strong electron-withdrawing trifluoromethyl groups could not lower an energy level of the  $\sigma^*$ -orbital of the C–O bond of **38**. An effort to exchange the counteranion for complete separation from the anion species is under way.

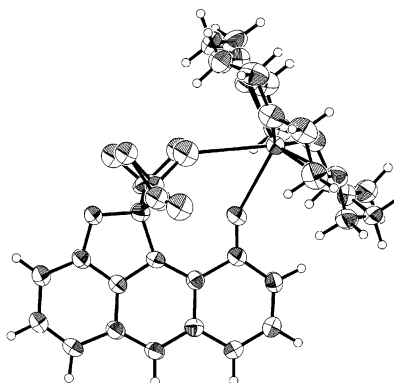
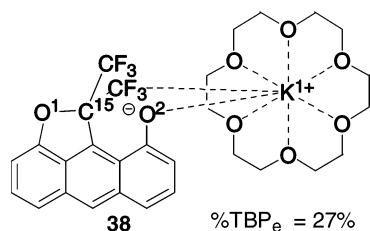
Thus, we have not yet been successful in obtaining an X-ray structure of a hypervalent pentacoordinate carbon compound having stronger apical C–O interaction bearing a formal minus charge. However, recently we could obtain hypervalent pentacoordinate boron compounds with a stronger B–O interaction. The results are described together with accurate X-ray analysis for a boron compound.

**Synthesis and Structures of Boron Compounds Bearing an Anthracene Skeleton.** As was already reported, boron compounds **50–52** bearing dimethylamino groups could be synthesized from **3** (Scheme 16).<sup>17d</sup> Single crystals of **50–52** suitable for X-ray analysis were obtained from a CH<sub>2</sub>Cl<sub>2</sub>–hexane solution. X-ray crystallographic analysis of **50–52** (Figure 9) showed the unsymmetrical structures with coordination of only one NMe<sub>2</sub> group toward the central boron atom. Shorter N–B bond lengths are 1.809(2) Å in **50**, 1.739(2) Å in **51**, and 1.667(3) Å in **52**, and the longer N–B bonds are 2.941–(2) Å in **50**, 3.124(3) Å in **51**, and 3.129(4) Å in **52**.

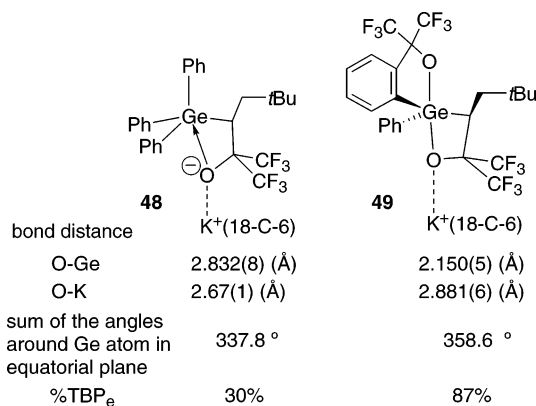
But the energy difference between the unsymmetrical tetra-coordinate structure and the symmetrical pentacoordinate one should be very small based on the variable temperature NMR. In <sup>1</sup>H NMR (CDCl<sub>3</sub> or CD<sub>2</sub>Cl<sub>2</sub>), **50–52** showed symmetrical

(41) (a) Kawashima, T.; Iwama, N.; Tokitoh, N.; Okazaki, R. *J. Org. Chem.* **1994**, *59*, 491–493. (b) Kawashima, T.; Nishiwaki, Y.; Okazaki, R. *J. Organomet. Chem.* **1995**, *499*, 143–146. (c) Kawashima, T. *J. Organomet. Chem.* **2000**, *611*, 256–263.

(40) Tamao, K.; Hayashi, T.; Ito, Y. *Organometallics* **1992**, *11*, 182–191.

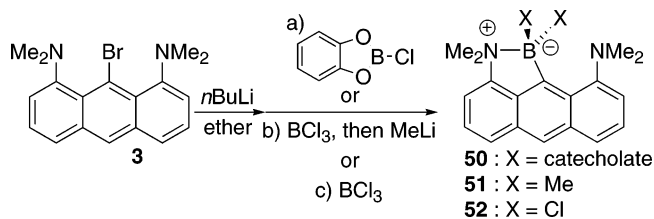


**Figure 7.** ORTEP drawing of **38** (30% thermal ellipsoid). Selected interatomic distances (Å) and angles (deg): C<sup>15</sup>–O<sup>1</sup> 1.470(5), C<sup>15</sup>–O<sup>2</sup> 2.991(5), K<sup>1</sup>–O<sup>2</sup> 2.570(3). Two of four disordered trifluoromethyl groups were omitted for clarification.

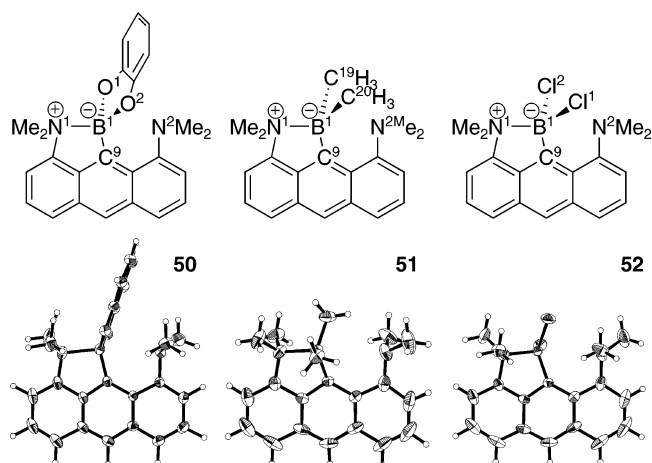


**Figure 8.** Interaction between an oxygen atom and potassium atom in hypervalent germanium complexes.

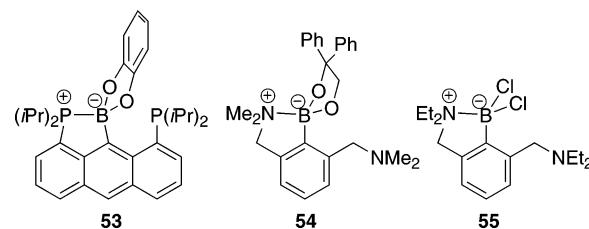
**Scheme 16.** Introduction of Boron Atom to the 9-Position of 1,8-Bis(dimethylamino)Anthracene



anthracene patterns in the aromatic region (two kinds of doublets, a triplet, and a singlet) and a sharp singlet signal of the two NMe<sub>2</sub> groups at room temperature. The peaks maintained their sharpness and the symmetrical pattern even at –80 °C. This is the case even in the most unsymmetrical dichloro compound **52** (CD<sub>2</sub>Cl<sub>2</sub>). It was similar to the behavior of **54** (Figure 10)<sup>9</sup> in <sup>1</sup>H NMR, which showed only one singlet (12H) of the two NMe<sub>2</sub> groups and maintained its sharpness in CD<sub>2</sub>Cl<sub>2</sub> from 25 °C to –100 °C. However, it was contrasted with the behavior of BCl<sub>2</sub>[2,6-(Et<sub>2</sub>NCH<sub>2</sub>)<sub>2</sub>C<sub>6</sub>H<sub>3</sub>] (**55**, Figure 10)<sup>45</sup> in <sup>1</sup>H NMR, which showed two kinds of NEt<sub>2</sub> groups in C<sub>6</sub>D<sub>6</sub> or THF-*d*<sub>8</sub> solvents at 25 °C. The NMR data of **52** indicates that the very rapid “bond-switching” accompanied with the inversion at the central atom (bell-clapper rearrangement)<sup>12</sup> is taking place in solution as illustrated in Scheme 17. Since the energy barrier



**Figure 9.** ORTEP drawing of **50–52** (30% thermal ellipsoid). Selected interatomic distances (Å) and angles (deg): (**50**) N<sup>1</sup>–B<sup>1</sup> 1.809(2), N<sup>2</sup>–B<sup>1</sup> 2.941(2), C<sup>9</sup>–B<sup>1</sup> 1.599(2), O<sup>1</sup>–B<sup>1</sup> 1.448(2), O<sup>2</sup>–B<sup>1</sup> 1.460(2), O<sup>1</sup>–B<sup>1</sup>–O<sup>2</sup> 107.5(1), O<sup>1</sup>–B<sup>1</sup>–N<sup>1</sup> 104.3(1), O<sup>1</sup>–B<sup>1</sup>–N<sup>2</sup> 75.96(8), O<sup>1</sup>–B<sup>1</sup>–C<sup>9</sup> 122.1(9), O<sup>2</sup>–B<sup>1</sup>–N<sup>1</sup> 106.4(1), O<sup>2</sup>–B<sup>1</sup>–N<sup>2</sup> 83.99(8), O<sup>2</sup>–B<sup>1</sup>–C<sup>9</sup> 116.6(1), N<sup>1</sup>–B<sup>1</sup>–N<sup>2</sup> 168.7(1), N<sup>1</sup>–B<sup>1</sup>–C<sup>9</sup> 97.4(1), N<sup>2</sup>–B<sup>1</sup>–C<sup>9</sup> 73.48(8). (**51**) N<sup>1</sup>–B<sup>1</sup> 1.739(2), N<sup>2</sup>–B<sup>1</sup> 3.124(3), C<sup>9</sup>–B<sup>1</sup> 1.646(2), C<sup>19</sup>–B<sup>1</sup> 1.609(3), C<sup>20</sup>–B<sup>1</sup> 1.622(3), N<sup>1</sup>–B<sup>1</sup>–N<sup>2</sup> 154.3(1), N<sup>1</sup>–B<sup>1</sup>–C<sup>9</sup> 96.7(1), N<sup>1</sup>–B<sup>1</sup>–C<sup>19</sup> 105.5(1), N<sup>1</sup>–B<sup>1</sup>–C<sup>20</sup> 108.3(1), N<sup>2</sup>–B<sup>1</sup>–C<sup>9</sup> 67.67(8), N<sup>2</sup>–B<sup>1</sup>–C<sup>19</sup> 72.3(1), N<sup>2</sup>–B<sup>1</sup>–C<sup>20</sup> 95.9(1), C<sup>9</sup>–B<sup>1</sup>–C<sup>19</sup> 127.0(2), C<sup>9</sup>–B<sup>1</sup>–C<sup>20</sup> 106.3(1), C<sup>19</sup>–B<sup>1</sup>–C<sup>20</sup> 111.1(1). (**52**) N<sup>1</sup>–B<sup>1</sup> 1.667(3), N<sup>2</sup>–B<sup>1</sup> 3.129(4), C<sup>9</sup>–B<sup>1</sup> 1.621(3), Cl<sup>1</sup>–B<sup>1</sup> 1.877(3), Cl<sup>2</sup>–B<sup>1</sup> 1.834(3), Cl<sup>1</sup>–B<sup>1</sup>–Cl<sup>2</sup> 107.8(1), Cl<sup>1</sup>–B<sup>1</sup>–N<sup>1</sup> 108.1(2), Cl<sup>1</sup>–B<sup>1</sup>–N<sup>2</sup> 97.9(1), N<sup>1</sup>–B<sup>1</sup>–N<sup>2</sup> 153.5(2), N<sup>1</sup>–B<sup>1</sup>–C<sup>9</sup> 99.9(2), N<sup>2</sup>–B<sup>1</sup>–C<sup>9</sup> 66.9(1).



**Figure 10.** Tetracoordinate borate bearing intramolecular coordination.

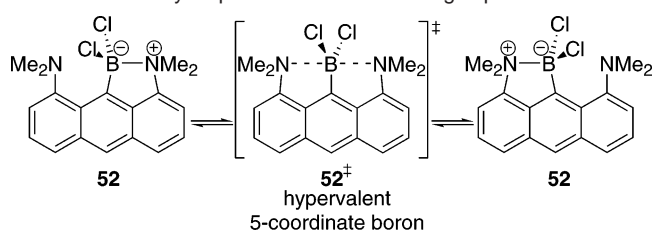
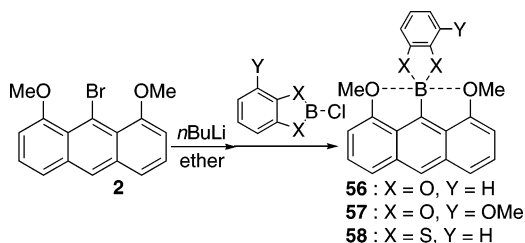
of the N–B bond-switching process in **52** was too small to measure by the coalescence method, the energy difference between the unsymmetrical tetracoordinate dichloroboron **52** and the pentacoordinate one **52**<sup>‡</sup>, which should be the transition state of the bond switching process, must be very small. The small activation energy in **52** indicates that our newly prepared rigid anthracene ligand system stabilizes the pentacoordinate dichloroboron transition state (**52**<sup>‡</sup>).

(42) Farfan, N.; Contreras, R. *J. Chem. Soc., Perkin Trans. 2* **1987**, 771–773.

(43) (a) Coppens, P. *X-ray Charge Densities and Chemical Bonding*; Oxford University Press: New York, 1997. (b) Wilson, A. J. C. *International Tables for Crystallography, Vol. C*; Kluwer Academic Publishers: Dordrecht, 1992.

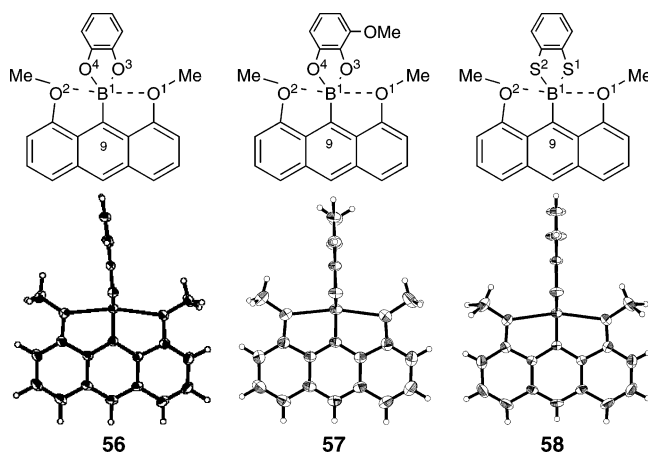
(44) Sana, M.; Leroy, G.; Wilante, C. *Organometallics* **1992**, *11*, 781–787.

(45) Schlenger, R.; Sieler, R.; Hey-Hawkins, E. *Main Group Chem.* **1997**, *2*, 141–148.

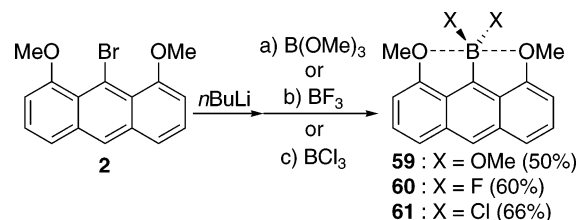
**Scheme 17.** Very Rapid N–B Bond-Switching Equilibrium in **52****Scheme 18.** Introduction of Boron Groups to the 9-Position of 1,8-Dimethoxyanthracene

In contrast to the NMe<sub>2</sub> ligand system, the corresponding boron compounds with the OMe-ligand system showed penta-coordinate structures except **61** (vide infra). The synthesis of the boron compounds **56–58** is straightforward as illustrated in Scheme 18. All of these compounds showed a symmetrical anthracene pattern (two doublets, a triplet and a singlet) and a very sharp singlet for the two OMe groups (6H), which indicated that the two OMe groups were equivalent in their <sup>1</sup>H NMR spectra. The <sup>11</sup>B NMR spectra of the compounds **56** ( $\delta$  28–39), **57** ( $\delta$  30–37), and **58** ( $\delta$  55–68) showed a broad peak over the range of normal catecholborane derivatives (cf. phenylcatecholborane:  $\delta$  = 32.1 in THF),<sup>42</sup> indicating that the interaction between the central boron atom and the oxygen atoms at the 1,8-positions is very weak. In contrast, upfield shifts were observed in the <sup>11</sup>B NMR spectra of the boron compounds prepared by Lee and Martin (–20 to –41 ppm).<sup>16</sup> The difference in the chemical shifts between the compounds of Lee and Martin and **56–58** may be a consequence of the charge difference (the former being anionic systems, while **56–58** are electronically neutral systems). Single crystals of **56–58** suitable for X-ray analysis were obtained by recrystallization from CH<sub>2</sub>Cl<sub>2</sub>/*n*-hexane (Figure 11). The sum of the bond angles around the central boron atom of **56–58** is 360.0°, which indicates that the central boron atom is planar with sp<sup>2</sup> hybridization. Thus, one of the lone pairs on the oxygen atoms at the 1,8-positions in **56–58** interacts with the empty p orbital of the central boron atom, which can be regarded as a slightly distorted TBP structure. The two B–O lengths (B1–O1, B1–O2) are 2.379(2) and 2.441(2) Å in **56**, 2.398(4) and 2.412(4) Å in **57**, and identical (2.436(2) Å) in **58**. The lengths are longer than those of the B1–O3 and B1–O4 (1.397(2) and 1.403(2) Å in **56**, 1.394(3) and 1.400(3) Å in **57**) but shorter than the sum of the van der Waals radii (3.48 Å).<sup>7</sup> The small difference in the B1–O1/2 distances observed in **56** may be a consequence of a packing effect or may be related to the electrophilicity of the central boron atom, since **57**, which bears a more electron-donating OMe substituent, exhibited a more symmetrical structure.

For further derivatization, **59–61** were synthesized as shown in Scheme 19. All of these compounds showed a symmetrical anthracene pattern (two doublets, a triplet and a singlet) and a



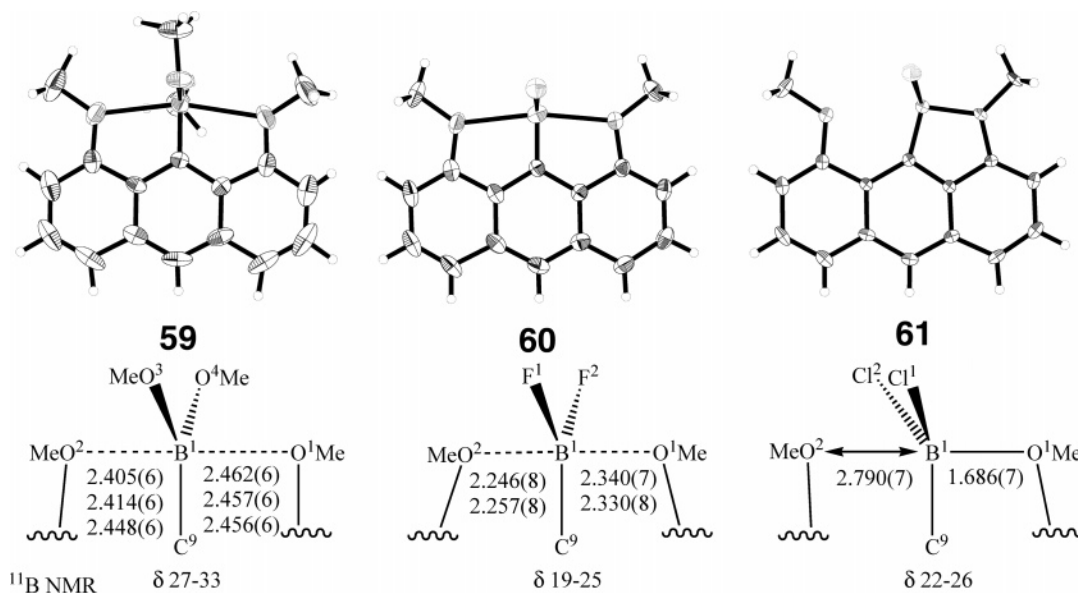
**Figure 11.** ORTEP drawing of **56–58** (30% thermal ellipsoid). Selected bond distances (Å) and angles (deg): (**56**) O<sup>2</sup>–B<sup>1</sup> 2.379(2), O<sup>1</sup>–B<sup>1</sup> 2.441(2), O<sup>3</sup>–B<sup>1</sup> 1.403(2), O<sup>4</sup>–B<sup>1</sup> 1.397(2), C<sup>9</sup>–B<sup>1</sup> 1.569(2), O<sup>1</sup>–B<sup>1</sup>–O<sup>2</sup> 167.10(7), O<sup>2</sup>–B<sup>1</sup>–O<sup>3</sup> 92.14(8), O<sup>2</sup>–B<sup>1</sup>–O<sup>4</sup> 92.65(8), O<sup>2</sup>–B<sup>1</sup>–C<sup>9</sup> 84.31(8), O<sup>1</sup>–B<sup>1</sup>–O<sup>3</sup> 95.59(8), O<sup>1</sup>–B<sup>1</sup>–O<sup>4</sup> 94.18(8), O<sup>1</sup>–B<sup>1</sup>–C<sup>9</sup> 82.79(8), O<sup>3</sup>–B<sup>1</sup>–O<sup>4</sup> 111.1(1), O<sup>3</sup>–B<sup>1</sup>–C<sup>9</sup> 125.4(1), O<sup>4</sup>–B<sup>1</sup>–C<sup>9</sup> 123.5(1). (**57**) O<sup>1</sup>–B<sup>1</sup> 2.398(4), O<sup>2</sup>–B<sup>1</sup> 2.412(4), O<sup>3</sup>–B<sup>1</sup> 1.394(3), O<sup>4</sup>–B<sup>1</sup> 1.400(3), C<sup>9</sup>–B<sup>1</sup> 1.570(4), O<sup>1</sup>–B<sup>1</sup>–O<sup>2</sup> 166.3(2), O<sup>1</sup>–B<sup>1</sup>–O<sup>3</sup> 96.3(2), O<sup>1</sup>–B<sup>1</sup>–O<sup>4</sup> 92.7(2), O<sup>1</sup>–B<sup>1</sup>–C<sup>9</sup> 83.3(2), O<sup>2</sup>–B<sup>1</sup>–O<sup>3</sup> 93.9(2), O<sup>2</sup>–B<sup>1</sup>–O<sup>4</sup> 92.1(2), O<sup>2</sup>–B<sup>1</sup>–C<sup>9</sup> 83.4(2), O<sup>3</sup>–B<sup>1</sup>–O<sup>4</sup> 111.3(2), O<sup>3</sup>–B<sup>1</sup>–C<sup>9</sup> 123.3(0), O<sup>4</sup>–B<sup>1</sup>–C<sup>9</sup> 125.4(2). (**58**) O<sup>1</sup>–B<sup>1</sup> 2.436(2), O<sup>2</sup>–B<sup>1</sup> 2.436(2), C<sup>9</sup>–B<sup>1</sup> 1.590(6), S<sup>1</sup>–B<sup>1</sup> 1.816(5), S<sup>2</sup>–B<sup>1</sup> 1.809(4), S<sup>1</sup>–B<sup>1</sup>–S<sup>2</sup> 112.4(3), S<sup>1</sup>–B<sup>1</sup>–O<sup>1</sup> 95.6(1), S<sup>1</sup>–B<sup>1</sup>–C<sup>9</sup> 121.1(3), S<sup>2</sup>–B<sup>1</sup>–O<sup>1</sup> 93.1(1), S<sup>2</sup>–B<sup>1</sup>–C<sup>9</sup> 126.6(3), O<sup>1</sup>–B<sup>1</sup>–O<sup>2</sup> 164.0(3), O<sup>1</sup>–B<sup>1</sup>–C<sup>9</sup> 82.2(1).

**Scheme 19.** Introduction of the BX<sub>2</sub> Substituent to the 9-Position of 1,8-Dimethoxyanthracene

very sharp singlet for the two OMe groups (6H) in their <sup>1</sup>H NMR spectra ( $\delta$  4.08 for **59**, 4.16 for **60** and 4.31 for **61**). The <sup>11</sup>B NMR spectra of **59–61** showed a broad signal in the same range ( $\delta$  27–33 for **59**, 20–24 for **60** and 22–25 for **61**).

Single crystals of **59–61** suitable for X-ray analysis were obtained from CH<sub>2</sub>Cl<sub>2</sub>/*n*-hexane solution. X-ray crystallographic analysis of **59–61** (Figure 12) showed very interesting results. The structure of **59** was almost symmetrical, their B–O distances [2.44 Å; average of the three independent molecules] were similar to those of catechol derivatives **56–58**. Although the structure of **60** was also symmetrical, their B–O distances were shortened [2.29 Å; average of the two independent molecules]. On the other hand, the structure of **61** was quite unsymmetrical, and their B–O distances [1.686(7) and 2.790(7) Å] were similar to those of the derivatives **50–52** bearing the two NMe<sub>2</sub> groups at the 1,8-positions of anthracene. It is interesting to compare the sum of the B–O distances in **59–61**. The sum of the B–O distances of **59** was 4.881 Å (average), which was similar to the distance between the two hydrogen atoms at the 1,8-positions of nonsubstituted anthracene [4.92 Å]<sup>46</sup> and longer than the distance between the two oxygen atoms at the 1,8-positions of 1,8-dimethoxyanthracene **6** [4.752(3) Å].

(46) (a) Brock, C. P. *Acta Crystallogr., Sect. B* **1990**, *46*, 795. (b) Mason, R. *Acta Crystallogr.* **1964**, *17*, 547–555.



**Figure 12.** ORTEP drawing (30% thermal ellipsoid; two (for **59**) or one (for **60**) independent molecules are omitted for clarity; B–O distances are described in Å) and  $^{11}\text{B}$  NMR chemical shift of **59**–**61**. Selected interatomic distances (Å) and angles (deg) are shown for the first molecule: (**59**) O<sup>1</sup>–B<sup>1</sup> 2.462(7), O<sup>2</sup>–B<sup>1</sup> 2.405(6), O<sup>3</sup>–B<sup>1</sup> 1.362(7), O<sup>4</sup>–B<sup>1</sup> 1.354(7), C<sup>9</sup>–B<sup>1</sup> 1.602(8), O<sup>1</sup>–B<sup>1</sup>–O<sup>2</sup> 164.3(3), O<sup>1</sup>–B<sup>1</sup>–O<sup>3</sup> 92.5(3), O<sup>1</sup>–B<sup>1</sup>–O<sup>4</sup> 95.0(3), O<sup>1</sup>–B<sup>1</sup>–C<sup>9</sup> 81.3(3), O<sup>2</sup>–B<sup>1</sup>–O<sup>3</sup> 95.2(4), O<sup>2</sup>–B<sup>1</sup>–O<sup>4</sup> 93.1(3), O<sup>2</sup>–B<sup>1</sup>–C<sup>9</sup> 83.0(3), O<sup>3</sup>–B<sup>1</sup>–O<sup>4</sup> 119.0(5), O<sup>3</sup>–B<sup>1</sup>–C<sup>9</sup> 117.4(4), O<sup>4</sup>–B<sup>1</sup>–C<sup>9</sup> 123.6(5). (**60**) F<sup>1</sup>–B<sup>1</sup> 1.344(7), F<sup>2</sup>–B<sup>1</sup> 1.308(7), O<sup>2</sup>–B<sup>1</sup> 2.246(8), O<sup>1</sup>–B<sup>1</sup> 2.340(7), C<sup>9</sup>–B<sup>1</sup> 1.582(6), F<sup>1</sup>–B<sup>1</sup>–F<sup>2</sup> 114.3(4), F<sup>1</sup>–B<sup>1</sup>–O<sup>2</sup> 94.2(4), F<sup>1</sup>–B<sup>1</sup>–O<sup>1</sup> 91.9(4), F<sup>1</sup>–B<sup>1</sup>–C<sup>9</sup> 122.7(5), F<sup>2</sup>–B<sup>1</sup>–O<sup>2</sup> 94.7(4), F<sup>2</sup>–B<sup>1</sup>–O<sup>1</sup> 93.2(4), F<sup>2</sup>–B<sup>1</sup>–C<sup>9</sup> 122.9(5), O<sup>2</sup>–B<sup>1</sup>–O<sup>1</sup> 167.0(3), O<sup>2</sup>–B<sup>1</sup>–C<sup>9</sup> 84.8(3), O<sup>1</sup>–B<sup>1</sup>–C<sup>9</sup> 82.3(3). (**61**) Cl<sup>1</sup>–B<sup>1</sup> 1.834(3), Cl<sup>2</sup>–B<sup>1</sup> 1.834(3), O<sup>1</sup>–B<sup>1</sup> 1.686(7), O<sup>2</sup>–B<sup>1</sup> 2.790(7), C<sup>9</sup>–B<sup>1</sup> 1.587(6), Cl<sup>1</sup>–B<sup>1</sup>–Cl<sup>2</sup> 112.0(3), Cl<sup>1</sup>–B<sup>1</sup>–O<sup>1</sup> 104.0(2), Cl<sup>1</sup>–B<sup>1</sup>–O<sup>2</sup> 82.8(2), Cl<sup>1</sup>–B<sup>1</sup>–C<sup>9</sup> 118.2(2), O<sup>1</sup>–B<sup>1</sup>–O<sup>2</sup> 167.4(3), O<sup>1</sup>–B<sup>1</sup>–C<sup>9</sup> 96.7(4), O<sup>2</sup>–B<sup>1</sup>–C<sup>9</sup> 70.7(3).

However, the sum of the B–O distances in **60** and **61** [4.59 Å for **60** and 4.48 Å for **61**] was shorter than the distance between the two oxygen atoms of 1,8-dimethoxyanthracene **6**, which may be due to the strong interaction between the central boron atom and the two oxygen atoms in **60** and even in **61**. Although all the structures of **59**–**61** were quite different, the  $^{11}\text{B}$  NMR chemical shifts of **59**–**61** are almost similar ( $\delta$  27–33 for **59**, 19–25 for **60**, and 22–26 for **61**). It may suggest that, in solution, the structures of these compounds are symmetric or rapid bond switching is taking place between O–B–O bonds.

**Comparison of X-ray Structures of the Carbon and Boron Compounds.** The distances between the central atom and the two coordinating atoms are summarized in Figure 13. In the case of the boron compounds, three types of structures were observed due to the difference of B–O distances, that is, loose pentacoordinate boron compounds (two relatively long and almost equivalent B–O lengths; **56**–**58** and **59**), a tight pentacoordinate boron compound (two relatively short and almost equivalent B–O lengths; **60**), and tetracoordinate boron compounds (two very different B–O (or N) lengths; **61**, **50**–**52**). In loose pentacoordinate boron compounds (**56**–**59**), the B–O distances were similar to the 1,9-peri-distance (2.46(2) Å)<sup>46</sup> of nonsubstituted anthracene and slightly longer than the distance between the two oxygen atoms of 1,8-dimethoxyanthracene **6**. The distances indicate that the B–O interaction was relatively weak. In tight pentacoordinate boron compound **60**, the B–O distances were clearly shorter than that of the loose one and the distance between the two oxygen atoms of 1,8-dimethoxyanthracene **6**. These apparently short B–O distances of **60** may prove that the B–O hypervalent interaction of **60** is strengthened from loose pentacoordinate species and the hypervalent interaction exists. In tetracoordinate boron compounds (**50**–**52** and **61**), the shorter B–O (or N) lengths were similar to the sum of the covalent radii;<sup>7</sup> on the other hand, the longer

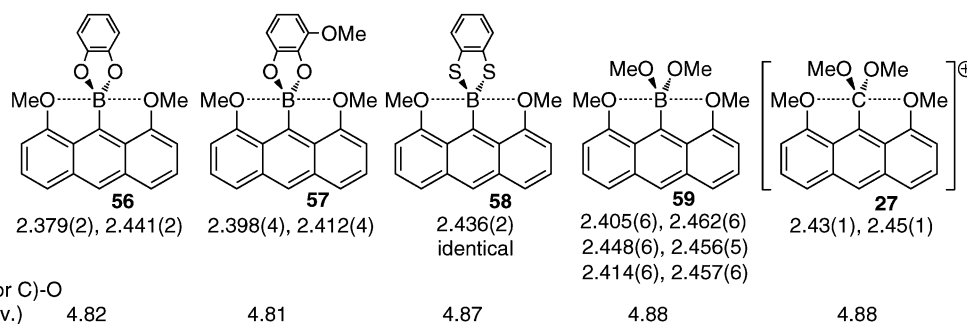
B–O (or N) lengths were slightly shorter than the sum of van der Waals radii or close to the sum. These distances indicate that one of two OMe (or NMe<sub>2</sub>) groups interacted strongly with the central boron atom, and the other one interacted very weakly with the central boron atom or did not interact at all. Based on the classification by bond lengths and configuration of the central boron atom, our carbon compounds **27** and **38** were classified as a loose pentacoordinate group and tetracoordinate group, respectively.

The apparent difference between the oxygen-donating skeleton and the nitrogen-donating one is probably due to the stronger stabilizing energy by the formation of one B–N bond in comparison with that of one B–O bond. Hence, the large stabilizing energy of the B–N bond overrides the destabilizing energy by the formation of the strained five-membered tetracoordinate boron structure. The F<sub>3</sub>B–NMe<sub>3</sub> bonding energy (26.6 kcal/mol) was reported to be much stronger than the corresponding F<sub>3</sub>B–OMe<sub>2</sub> bonding energy (13.9 kcal/mol).<sup>44</sup>

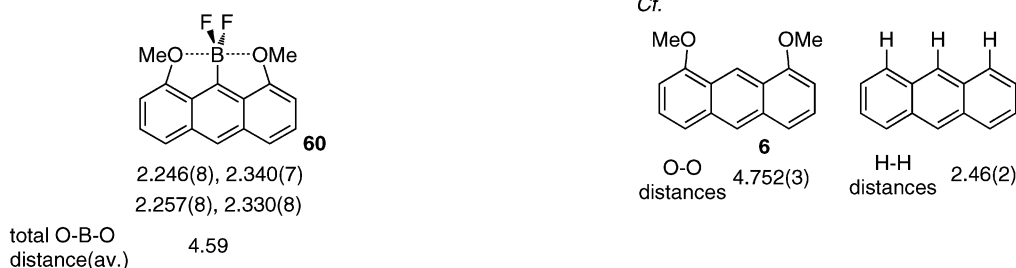
The difference among the OMe, F, and Cl (**59**, **60**, and **61**) in the oxygen-donating ligand can be explained by a similar delicate balance between the stabilizing energy by the formation of two relatively weak B–O bonds and the stabilizing energy by the formation of one strong B–O bond and the destabilizing energy by pyramidalization. It has been well established by several different experimental methods that the Lewis acidities of the boron trihalides are in the order of BF<sub>3</sub> < BCl<sub>3</sub> < BBr<sub>3</sub>.<sup>47</sup> This order is contrary to the expectation based on the electronegativity among F, Cl, and Br, which predicts that a positive charge density on boron decreases in the order BF<sub>3</sub> > BCl<sub>3</sub> > BBr<sub>3</sub>. In addition, theoretical calculation supported the trend

(47) (a) Brown, H. C.; Holmes, R. R. *J. Am. Chem. Soc.* **1956**, *78*, 2173–2176. (b) Shriver, D. F.; Swanson, B. *Inorg. Chem.* **1971**, *10*, 1354–1365. (c) Cotton, F. A.; Wilkinson, G. *Advanced Inorganic Chemistry*; John Wiley and Sons: New York, 1980.

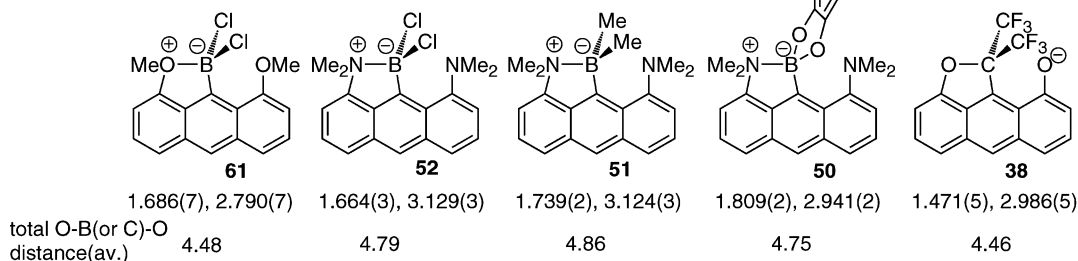
## loose pentacoordinate



## tight pentacoordinate

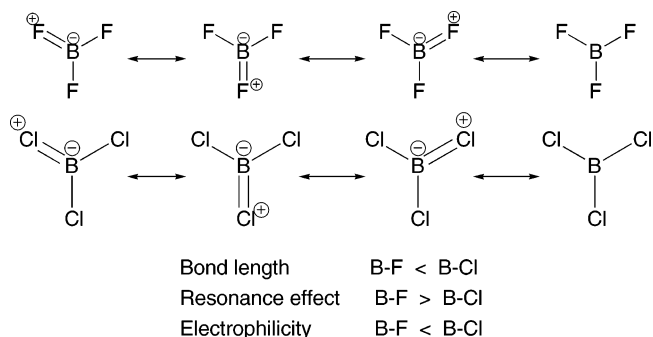


## tetracoordinate



**Figure 13.** Classification of the 9-boron and 9-carbon compounds of anthracenes based on the X-ray structures.

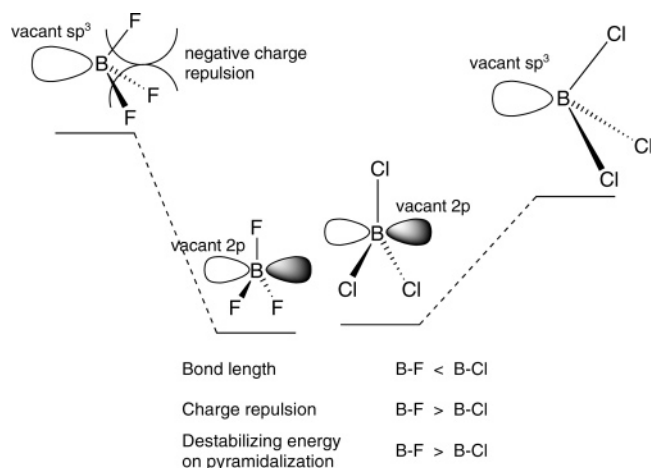
of the charge density of the central boron atom, which is consistent with the electronegativity.<sup>48</sup> The generally accepted explanation for the anomalous order of Lewis acidity is based on the strong back-donation of electrons from one of the lone pairs (2p orbital) of the fluorine atom to the vacant 2p<sub>z</sub> orbital of the boron atom, which leads to some double-bond character for the B–F bond in BF<sub>3</sub> (Figure 14).<sup>47,49</sup> In BCl<sub>3</sub> and BBr<sub>3</sub>, this type of back-donation is much less important because the longer B–Cl and B–Br bonds form a poorer overlap. These results suggest that the oxygen and the fluorine substituents donate electrons toward the central boron atom stronger than the chlorine substituent. Indeed, in the case of **59** and **60**, both averages of the B–X distances [1.36 Å, for **59**, X = OMe; 1.34 Å, for **60**, X = F] were 88% of the sum of the covalent radii (1.54 Å for B–O; 1.52 Å for B–F),<sup>7</sup> while the B–Cl distance (1.83 Å, identical) of **61** was essentially the same (98%) as the sum of the covalent radius (1.87 Å for B–Cl).<sup>7</sup> However, the Brinck group suggested that the back-donation was not essentially important based on the data of the coefficient of HOMO, which corresponded to the pπ–pπ interaction between



**Figure 14.** Resonance effect on BX<sub>3</sub>.

B and X.<sup>48a</sup> They concluded that the Lewis acidity of BX<sub>3</sub> was related to their destabilization energy on the pyramidalization, which was defined as the energy difference between the sp<sup>2</sup> and assumed sp<sup>3</sup> state of BX<sub>3</sub> and not related to the charge density of the central boron atom. That is, an increasing electronegativity from Br to Cl to F should increase the polarity of the B–X bond. As a result, in addition to the effect of B–X bond lengths, the repulsion among the partial negative charge of X should increase from Br to Cl to F when BX<sub>3</sub> is pyramidalized because X comes closer to each other in sp<sup>3</sup> configuration (Figure 15).

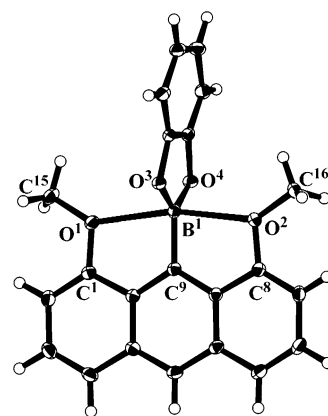
(48) (a) Brinck, T.; Murray, J. S.; Politzer, P. *Inorg. Chem.* **1993**, *32*, 2622–2625. (b) Robinson, E. A.; Johnson, S. A.; Tang, T.-H.; Gillespie, R. J. *Inorg. Chem.* **1997**, *36*, 3022–3030. (c) Robinson, E. A.; Heard, G. L.; Gillespie, R. J. *J. Mol. Struct.* **1999**, *485*, 305–319.  
(49) Pearson, R. G. *Inorg. Chem.* **1988**, *27*, 734–740.



**Figure 15.** Destabilization of  $BX_3$  species on their pyramidalization.

In our compounds **60** and **61** (Figures 12 and 13), the rigidity of the boron  $sp^2$  plane of **60** may be stronger than that of **61** because of the repulsion of the partial negative charge in pyramidalization, too. In consequence, **61** was pyramidalized to obtain a larger stabilization energy by the formation of a single bond between the central boron atom and the oxygen atom, while **60** kept its planarity of the  $sp^2$  plane because the stabilization energy by the formation of a single bond is not large enough to overcome the destabilization energy of pyramidalization. In the case of **59** and **60**, the planarity of **59** was strong probably due to the same reason as that of **60**. However, a difference in the electronegativity between the fluorine atom and the methoxy group leads to the difference in the partial positive charge of the central boron atom, which directly affects the strength of the apical B–O interaction. Because of the reason for the formation of tight pentacoordinate boron compounds, the synthesis of tight pentacoordinate carbon compounds bearing some electron-withdrawing groups is currently under investigation.

**Experimental Electron Density Distribution Analysis of 56.** The structure of **56** obtained from the accurate X-ray analysis (see Experimental Section) was slightly unsymmetrical [B–O distances are 2.3780(9) Å for B–O<sup>2</sup> and 2.4367(9) Å for B–O<sup>1</sup>] and is similar to the regular X-ray analysis described above [B–O distances are 2.379(2) and 2.441(2) Å]. The molecular structure and static model maps of **56** are shown in Figures 16 and 17, respectively. The central boron atom forms three valence bonds with C<sup>9</sup>, O<sup>3</sup>, and O<sup>4</sup> and two short contacts with O<sup>1</sup> and O<sup>2</sup> to form a trigonal bipyramidal structure, which is elongated along the O<sup>1</sup>–B<sup>1</sup>–O<sup>2</sup> direction. The covalent characters of the former three bonds are illustrated by the electron-rich regions on the intermediate of the bonds in the static model map on the catechol moiety (Figure 17b). The central boron atom is placed on the trigonal plane formed by the three atoms, and the sum of the angles around the B atom is 360°. The geometry indicates the  $sp^2$  hybridization of the central boron atom. The  $sp^2$  plane is almost perpendicular to the anthracene plane. The atoms O<sup>1</sup> and O<sup>2</sup> are placed at the apical positions of the bipyramid formed around the central boron atom, and the B–O distances (av 2.407 Å) are significantly shorter than the sum of the van der Waals radii, 3.48 Å.<sup>7</sup> In the two methoxy groups on the 1- and 8-positions, the angles C<sup>1</sup>–O<sup>1</sup>–C<sup>15</sup> and C<sup>8</sup>–O<sup>2</sup>–C<sup>16</sup> are close to 120°. These suggest the  $sp^2$  hybridization of the two O atoms.

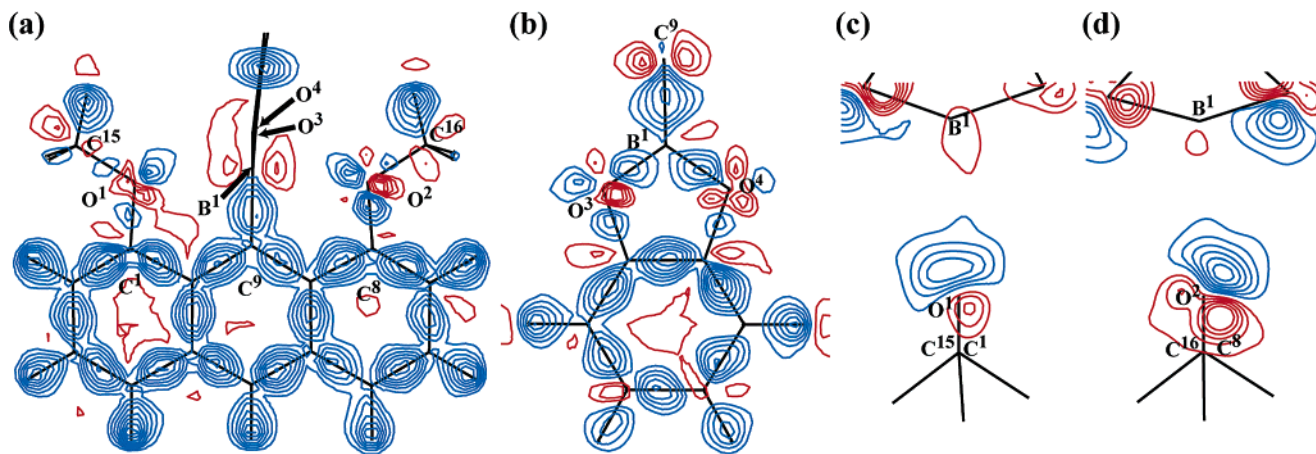


**Figure 16.** Molecular structure of **56** with the atom-labeling scheme. Displacement ellipsoids are drawn at the 50% probability level, and H atoms are shown as small spheres of arbitrary radii. The data of the conventional refinement using data of  $\sin \theta/\lambda \leq 0.65 \text{ \AA}^{-1}$  were used for the preparation of the figure.

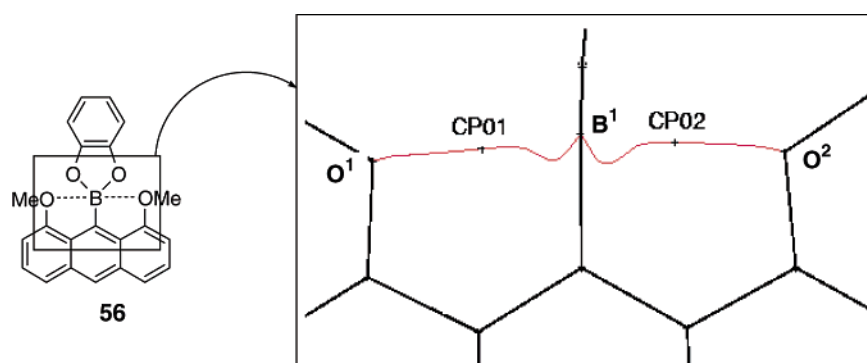
Since the atoms B<sup>1</sup>, O<sup>1</sup>, O<sup>2</sup>, C<sup>15</sup>, and C<sup>16</sup> are coplanar to the anthracene plane and the conformations of the methoxy groups are anti to the central boron atom, one of the two lone pairs on each O atom is directed and should be coordinated to the empty 2p orbital on the boron atom and the other should be parallel to  $\pi$  electrons of the anthracene skeleton.

The character of the B–O bonds is clearly shown in the static model maps (Figure 17).<sup>43</sup> The topology of the electron density distributions is quite different from those of covalent bonds. As shown in Figure 17c and d, the lone pairs on each O atom appeared in the plane bisecting C–O–C as single peaks. The peaks are extended to the central boron atom and diffused perpendicular to the C–O–C planes. The shapes of the peaks are due to the overlap of the two lone pairs accommodated in one of the  $sp^2$  and p orbitals which are directed along the bisection of the C–O–C angle and perpendicular to the C–O–C plane, respectively. As shown in Figure 17a, the hole of the 2p orbital appeared as electron-deficient regions at both sides of the central boron atom and has lobes extended perpendicular to the  $sp^2$  plane. The lone pairs in the  $sp^2$  orbital on each O atom are on a co-plane of the anthracene and directed to the empty 2p orbital of the B atom. Such geometry of the orbitals clearly indicates the electron donations from the lone pairs in the  $sp^2$  orbitals on the O atoms to the empty 2p orbital on the central boron atom to form a three-center four-electron bond.

For quantitative treatment of the characterization of the bonds, topological analyses were performed. The bond paths were found between the B–O bonds as shown in Figure 18. The shapes of the bond paths of the two bonds are almost identical. The bond critical points are also found on each bond path, and the points are closer to the central boron atom than the O atoms because of the polarities of the bonds. The small electron densities ( $\rho(\mathbf{r})$ : B<sup>1</sup>–O<sup>1</sup> 0.027(4), B<sup>1</sup>–O<sup>2</sup> 0.030(4)  $e/a_0^3$ ;  $a_0 = 0.529177 \text{ \AA}$ ) and the small positive Laplacian ( $\nabla^2(\mathbf{r})$ : B<sup>1</sup>–O<sup>1</sup> 0.050(2), B<sup>1</sup>–O<sup>2</sup> 0.052(2)  $e/a_0^5$ ) values at the bond critical points indicate the ionic character of the bonds. The difference of  $\rho(\mathbf{r})$  and  $\nabla^2(\mathbf{r})$  between B<sup>1</sup>–O<sup>1</sup> and B<sup>1</sup>–O<sup>2</sup> can be related to the difference between the bond lengths (B<sup>1</sup>–O<sup>1</sup> 2.4367(9) Å, B<sup>1</sup>–O<sup>2</sup> 2.3780(9) Å), since the decrease in the  $\rho(\mathbf{r})$  and  $\nabla^2(\mathbf{r})$  values may imply weakening of the bond. On the other hand, the bond ellipticity,  $\epsilon$ , values of the two B–O bonds are quite different



**Figure 17.** Static model maps of **56** on (a) the anthracene plane, (b) the plane of catechol moiety, (c) the plane bisecting  $C^1-O^1-C^{15}$ , and (d) the plane bisecting  $C^8-O^2-C^{16}$ . Contour interval is  $0.1 e \text{ \AA}^{-3}$ . Positive and negative regions are shown as blue and red lines, respectively, and zero contours are omitted.



**Figure 18.** Bond paths of the  $B^1-O^1$  and  $B^1-O^2$  bonds of **56** obtained by the accurate X-ray analysis. Bond paths are shown as red lines.

( $\epsilon$ :  $B^1-O^1$  0.29,  $B^1-O^2$  0.77). The difference in the  $\epsilon$  values indicates that the donation from the lone pair in the p orbital is more sensitive to the distance than those in the  $sp^2$  orbital because of the directionality of the p orbital on the two oxygen atoms. The orders of these values are in agreement with the results from the DFT calculation which shows the symmetrical structure ( $\rho(\mathbf{r})$ ,  $0.022 e/a_0^3$ ;  $\nabla^2(\mathbf{r})$ ,  $0.058 e/a_0^5$ ;  $\epsilon$ , 0.266) (vide infra).

These present the first evidence and characterization of the O–B–O three-center four-electron bond based on the experimental electron density distribution analysis.

**Elucidation of the Interaction between the Central Boron Atom and the Two Oxygen Atoms of **56**, **60**, and **61** Based on the DFT Calculation.** The attractive interaction between the central boron atom and the oxygen atoms at the 1,8-positions is also confirmed by hybrid density functional theory (DFT) at the B3PW91/6-31G(d) level using the Gaussian 98 program.<sup>32</sup> The optimized geometry of **56** is symmetrical (Figure 19b), where the two B–O bond lengths are identical (2.431 Å) and are slightly longer than the experimental data (2.3780(9) and 2.4367(9) Å). The topological analysis of **56** shows that the bond path is found between the central boron atom and the two oxygen atoms. The B–O bond is weak and slightly ionic as shown by the small value of the electron density [ $\rho(\mathbf{r})$ :  $0.022 e/a_0^3$ ] and the small positive Laplacian value [ $\nabla^2\rho(\mathbf{r})$ :  $0.058 e/a_0^5$ ] at the bond critical points. These values together with the large value of the ellipticity ( $\epsilon = 0.266$ ) are well consistent with the data from the accurate X-ray analysis and very similar

to the values for the C–O bond in our hypervalent pentacoordinate carbon compound **27** [ $\rho(\mathbf{r})$ ,  $0.022 e/a_0^3$ ;  $\nabla^2\rho(\mathbf{r})$ ,  $0.080 e/a_0^5$ ;  $\epsilon$ , 0.219] (Figure 19a). The calculation also showed that the symmetrical pentacoordinated structure was a global minimum in **60** (Figure 19c), but in **61** both the pentacoordinated structure and the tetracoordinated one were found as minima (Figure 19d). The tetracoordinate structure was only 0.14 and 1.24 kcal/mol more stable at the B3PW91/6-31G(d) and MP2/6-31G(d) levels, respectively, than the pentacoordinated one. It should be noted that the DFT calculation at the B3LYP/6-31G(d) level showed that the pentacoordinated structure was 0.63 kcal/mol more stable for **61**.

## Conclusion

Various carbon and boron compounds bearing a 1,8-disubstituted anthracene skeleton, such as **27**, **38**, **50–52**, **56–61**, were synthesized and characterized by X-ray analysis. They showed three types of the structures based on the kinds of substituents. The first one is symmetrical and a loose pentacoordinate structure, which has the  $sp^2$  boron and carbon atoms and the two weak apical interactions. The second one is an unsymmetrical tetracoordinate structure, which has the  $sp^3$  boron and carbon atoms. The third one is symmetrical and a tight pentacoordinate structure, which resulted from the special feature of the fluorine atoms. The existence of hypervalent interaction was proved by the Atoms In Molecules Theory, experimental electron density analysis, DFT calculation, and the comparison among the structures of tight and loose pentacoordinate



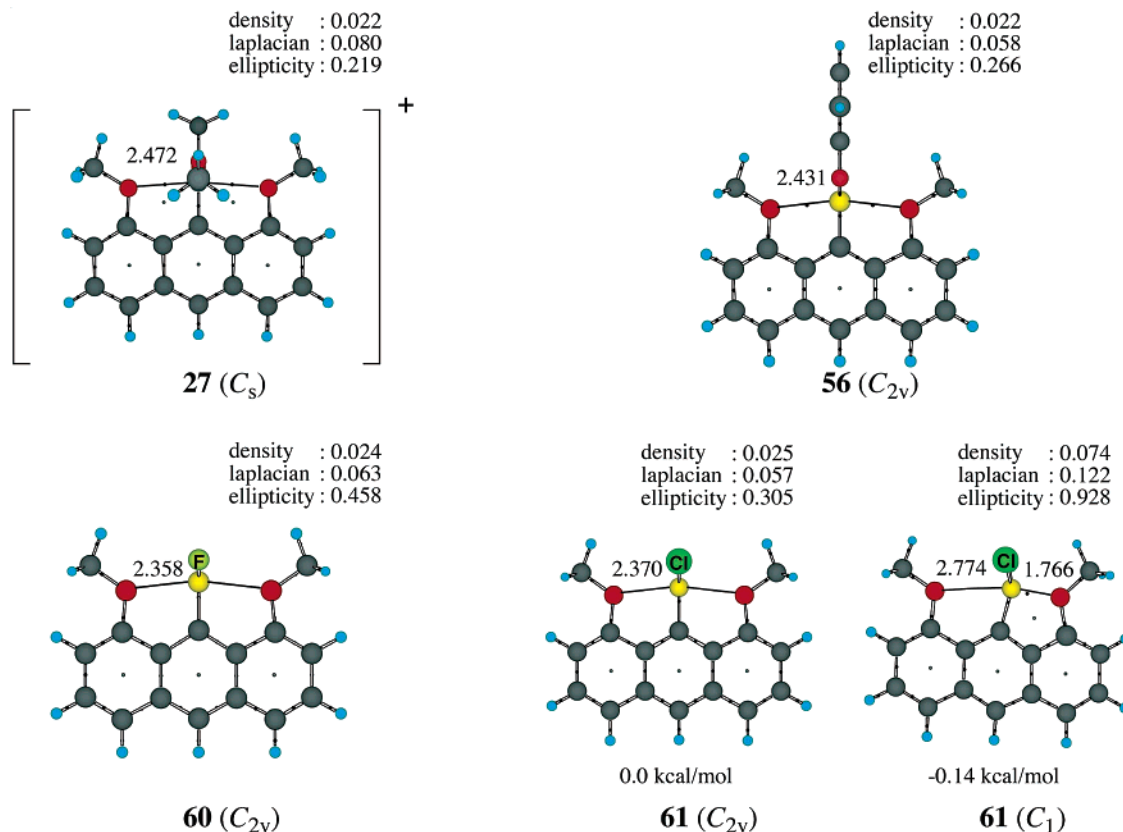


Figure 19. Optimized structures and the AIM data of **27**, **56**, **60**, and **61** at the B3PW91/6-31G(d) level.

species. Since these results showed us the scope for the isolation of tight pentacoordinate carbon species, further investigation toward the synthesis of tight-pentacoordinate carbon compounds is under way.

## Experimental Section

**General.** Ether and tetrahydrofuran were freshly distilled from sodium benzophenone, and other solvents were distilled from calcium hydride under argon atmosphere. Merck silica gel 9385 and 7730 was used for column chromatography and preparative TLC. LC908-C60 (Japan Analytical Industry) with a 40  $\phi$  column was used for HPLC purification with  $\text{ClCH}_2\text{CH}_2\text{Cl}$  as an eluent. Melting points were taken on a Yanagimoto micromelting point apparatus.  $^1\text{H}$  NMR (400 MHz),  $^{11}\text{B}$  NMR (127 MHz),  $^{13}\text{C}$  NMR (99 MHz),  $^{19}\text{F}$  NMR (372 MHz), and  $^{31}\text{P}$  NMR (162 MHz) spectra were recorded on a JEOL EX-400 and an AL-400 spectrometer. Chemical shifts ( $\delta$ ) are reported as parts per million from internal  $\text{CHCl}_3$  for  $^1\text{H}$  ( $\delta$  7.26) or from external  $\text{BF}_3 \cdot \text{OEt}_2$  for  $^{11}\text{B}$  ( $\delta$  0.0) or from internal  $\text{CDCl}_3$  for  $^{13}\text{C}$  ( $\delta$  77.0) or from external  $\text{CFCl}_3$  for  $^{19}\text{F}$  ( $\delta$  0.0) or from external  $\text{H}_3\text{PO}_4$  for  $^{31}\text{P}$  ( $\delta$  0.0). Mass spectrometry was recorded on a JEOL SX-102A spectrometer. Elemental analysis was performed on a Perkin-Elmer 2400CHN elemental analyzer.

**Synthesis of 1,8,9-Tribromoanthracene 11.** To a mixture of 4,4'-di-*tert*-butylbiphenyl (2.70 g, 10 mmol) and Li (71.8 mg, 10 mmol) THF (10 mL) was added at 0  $^\circ\text{C}$  under Ar followed by stirring for 4 h at 0  $^\circ\text{C}$  with a glass-coated stirring bar to give LDBB (lithium 4,4'-di-*tert*-butylbiphenylide) solution. The solution of **9** (391 mg, 1 mmol) in THF (5 mL) was added to the LDBB solution at  $-78$   $^\circ\text{C}$  followed by stirring at  $-78$   $^\circ\text{C}$  for 1 h. This mixture was allowed to warm to  $-20$   $^\circ\text{C}$  and was stirred at that temperature for 2 h. At  $-20$   $^\circ\text{C}$ ,  $\text{BrCF}_2\text{-CF}_2\text{Br}$  (1.8 mL, 15 mmol) was added dropwise into the reaction mixture. This mixture was allowed to warm to rt and was stirred for 14 h. Solvents were removed from the reaction mixture under reduced

pressure. This crude product was dissolved in  $\text{CH}_2\text{Cl}_2$  and washed with  $\text{H}_2\text{O}$ . The organic layer was collected and dried over  $\text{K}_2\text{CO}_3$ . The solvents were removed under reduced pressure to give a crude product. This crude product was purified by column chromatography ( $\text{CH}_2\text{Cl}_2$ -hexane = 0:1-1:15) to give a yellow solid of **11** (88.2 mg, 21%). Single crystals suitable for X-ray analysis were obtained from  $\text{CH}_2\text{Cl}_2$ -hexane solution under air:  $^1\text{H}$  NMR (400 MHz, 25  $^\circ\text{C}$ ,  $\text{CDCl}_3$ )  $\delta$  7.29 (dd, 2H,  $J = 8$  Hz, 8 Hz), 7.96 (d, 2H,  $J = 8$  Hz), 8.01 (d, 2H,  $J = 8$  Hz), 8.40 (s, 1H); MS (FAB $^+$ )  $\text{M}^+ = 412, 414, 416, 418$ . Anal. Calcd for  $\text{C}_{14}\text{H}_7\text{Br}_3$ : C, 40.53; H, 1.70%. Found: C, 40.41; H, 1.42%.

**Improved Synthesis of 1,8-Dimethoxy-9-bromoanthracene 2 from 12.** To a mixture of lithium (880 mg, 127 mmol) and DTBB (4,4'-di-*tert*-butylbiphenyl; 33.6 g, 126 mmol) THF (300 mL) was added at 0  $^\circ\text{C}$ . The mixture was stirred with a glass-coated stirring bar at 0  $^\circ\text{C}$  until the lithium metal disappeared. Part (250 mL) of the generated LDBB solution (ca. 0.4 M, 250 mL, 100 mmol) was added to a solution of **12** (8.82 g, 25 mmol), and the mixture was stirred with a glass-coated stirring bar at  $-100$   $^\circ\text{C}$  for 10 min and allowed to warm to  $-41$   $^\circ\text{C}$ . After stirring for 15 min at  $-41$   $^\circ\text{C}$ ,  $\text{BrCF}_2\text{-CF}_2\text{Br}$  (12.3 mL, 100 mmol) was added dropwise to the reaction mixture at  $-41$   $^\circ\text{C}$ . The mixture was stirred for 10 min at  $-41$   $^\circ\text{C}$  and for an additional 3.5 h at rt. Silica gel (200 mL, measured by beaker) was added to the mixture, and the solvents were removed under reduced pressure. The crude product, which was carried on silica gel, was charged on column chromatography. Initially, hexane was used as an eluent to remove DTBB. After the elution of DTBB was complete, hexane was substituted to a mixture of  $\text{CH}_2\text{Cl}_2$  and hexane (0:1 ~ 1:3) gradually to give a yellow fraction of **2** (4.09 g, 51%); mp 141-149  $^\circ\text{C}$  (dec),  $^1\text{H}$  NMR (400 MHz, 25  $^\circ\text{C}$ ,  $\text{CDCl}_3$ )  $\delta$  4.04 (s, 6H), 6.90 (d, 2H,  $J = 8$  Hz), 7.36 (t, 2H,  $J = 8$  Hz), 7.54 (d, 2H,  $J = 8$  Hz), 8.26 (s, 1H);  $^{13}\text{C}$  NMR (100 MHz,  $\text{CDCl}_3$ , 25  $^\circ\text{C}$ )  $\delta$  55.75, 101.78, 116.19, 119.63, 121.33, 124.75, 127.37, 131.68, 155.77; MS (FAB $^+$ )  $\text{M}^+ = 316, 318$ .

Anal. Calcd for  $C_{16}H_{13}BrO_2$ : C, 60.59; H, 4.13%. Found: C, 60.50; H, 3.88%.

**Synthesis of 1,8-Dimethoxy-9-dimethoxyborylanthracene 59.** A solution of *n*-BuLi in *n*-hexane (0.7 mL, 1.1 mmol) was added dropwise to a solution of **2** (318 mg, 1 mmol) in ether (30 mL) at  $-100^\circ\text{C}$ . After the solution was stirred for 2 h at  $-100^\circ\text{C}$ ,  $B(OMe)_3$  (0.14 mL, 1.2 mmol) was added dropwise to the solution at  $-100^\circ\text{C}$ . The reaction mixture was slowly warmed to rt within 8 h. Aqueous HCl (1 N) was added to the mixture, and the mixture was extracted with  $CH_2Cl_2$ . Collected organic layer was dried and evaporated to give a crude product. The crude product was purified by HPLC (RT = 73 min) to 156 mg (50%) of **59**. Single crystals suitable for X-ray analysis and measurement of mp and  $^{13}\text{C}$  NMR were obtained from the  $CH_2Cl_2$ -*n*-hexane solution under Ar atmosphere;  $^1\text{H}$  NMR (400 MHz,  $CDCl_3$ ,  $25^\circ\text{C}$ )  $\delta$  3.45 (s, 6H), 4.08 (s, 6H), 6.75 (d, 2H,  $J = 8$  Hz), 7.37 (t, 2H,  $J = 8$  Hz), 7.58 (d, 2H,  $J = 8$  Hz), 8.32 (s, 1H);  $^{11}\text{B}$  NMR (127 MHz,  $CDCl_3$ ,  $25^\circ\text{C}$ )  $\delta$  27–33 (br);  $^{13}\text{C}$  NMR (99 MHz,  $CDCl_3$ ,  $25^\circ\text{C}$ )  $\delta$  51.94, 55.65, 102.04, 121.13, 125.16, 126.27, 127.46, 132.66, 156.34. Anal. Calcd for  $C_{18}H_{19}BO_4$ : C, 69.71; H, 6.17%. Found: C, 69.49; H, 6.20%.

**Synthesis of 1,8-Dimethoxy-9-difluoroborylanthracene 60.** A solution of *n*-BuLi in *n*-hexane (0.7 mL, 1.1 mmol) was added dropwise to a solution of **2** (317 mg, 1 mmol) in ether (50 mL) at  $-78^\circ\text{C}$ . After the solution was stirred for 1.5 h at  $-78^\circ\text{C}$ ,  $BF_3 \cdot OEt_2$  (0.14 mL, 1.1 mmol) was added dropwise to the solution at  $-78^\circ\text{C}$ . The reaction mixture was slowly warmed to rt within 3 h. After solvents were removed under reduced pressure,  $ClCH_2CH_2Cl$  soluble materials were injected into an HPLC column. A fraction at RT = 73 min was collected and concentrated to give 172 mg (60%) of **60**. Single crystals suitable for X-ray analysis and measurement of mp and  $^{13}\text{C}$  NMR were obtained from a  $CH_2Cl_2$ -*n*-hexane solution in a refrigerator; mp  $242$ – $252^\circ\text{C}$  (dec);  $^1\text{H}$  NMR (400 MHz,  $CDCl_3$ ,  $25^\circ\text{C}$ )  $\delta$  4.16 (s, 6H), 6.80 (d, 2H,  $J = 8$  Hz), 7.41 (t, 2H,  $J = 8$  Hz), 7.63 (d, 2H,  $J = 8$  Hz), 8.38 (s, 1H);  $^{11}\text{B}$  NMR (127 MHz,  $CDCl_3$ ,  $25^\circ\text{C}$ )  $\delta$  19–25 (br);  $^{13}\text{C}$  NMR (99 MHz,  $CDCl_3$ ,  $25^\circ\text{C}$ )  $\delta$  55.8, 102.0 (d,  $J_{CF} = 1.6$  Hz), 121.3, 125.51, 125.55, 126.3, 127.4 (d,  $J_{CF} = 1.7$  Hz), 132.1, 154.3;  $^{19}\text{F}$  NMR (372 MHz,  $CDCl_3$ ,  $25^\circ\text{C}$ )  $\delta$   $-96.3$  (s). Anal. Calcd for  $C_{16}H_{13}BF_2O_2$ : C, 67.17; H, 4.58%. Found: C, 66.86; H, 4.27%.

**Synthesis of 1,8-Dimethoxy-9-dichloroborylanthracene 61.** A solution of *n*-BuLi in *n*-hexane (1.4 mL, 1.1 mmol) was added dropwise to a solution of **2** (634 mg, 2 mmol) in ether (120 mL) at  $-78^\circ\text{C}$ . After the solution was stirred for 1.5 h at  $-78^\circ\text{C}$ , a solution of  $BCl_3$  in heptane (2.2 mL, 2.2 mmol) was added dropwise to the solution at  $-78^\circ\text{C}$ . The reaction mixture was warmed to rt within 1 h. After solvents were removed under reduced pressure,  $ClCH_2CH_2Cl$  soluble materials were injected into an HPLC column. A fraction at RT = 69 min was collected and concentrated to give 420 mg (60%) of **61** with small amounts of impurities. Single crystals suitable for X-ray analysis and measurement of mp and  $^{13}\text{C}$  NMR were obtained from a  $CH_2Cl_2$ -*n*-hexane solution in a refrigerator; mp  $142$ – $145^\circ\text{C}$  (dec);  $^1\text{H}$  NMR (400 MHz,  $CDCl_3$ ,  $25^\circ\text{C}$ )  $\delta$  4.31 (s, 6H), 6.83 (d, 2H,  $J = 8$  Hz), 7.42 (t, 2H,  $J = 8$  Hz), 7.67 (d, 2H,  $J = 8$  Hz), 8.34 (s, 1H);  $^{11}\text{B}$  NMR (127 MHz,  $CDCl_3$ ,  $25^\circ\text{C}$ )  $\delta$  22–25 (br);  $^{13}\text{C}$  NMR (99 MHz,  $CDCl_3$ ,  $25^\circ\text{C}$ )  $\delta$  55.4, 101.8, 122.0, 125.30, 125.32, 125.6, 125.8, 132.5, 154.4. Anal. Calcd for  $C_{16}H_{13}BCl_2O_2$ : C, 60.24; H, 4.11%. Found: C, 59.83; H, 4.00%.

**X-ray Crystallographic Analysis.** X-ray data, except experimental electron distribution analysis, were collected on a Mac Science DIP2030 imaging plate equipped with graphite-monochromated  $Mo\ K\alpha$  radiation ( $\lambda = 0.71073$  Å). The unit cell parameters were determined by autoindexing several images in each data set separately with the program DENZO. For each data set, rotation images were collected in  $3^\circ$  ( $6^\circ$  for **27**) increments with a total rotation of  $180^\circ$  about  $\phi$ . Data were processed by SCALEPACK. The structures, except **6** and **38**, were solved using the teXsan system and refined by full-matrix least-squares,

and the structures of **6** and **38** were solved using SIR97<sup>50</sup> and SHELXL97<sup>51</sup> and refined by full-matrix least-squares. Structures were drawn by the Oak Ridge Thermal Ellipsoid Plot program (ORTEP-III<sup>52</sup>). The programs DENZO and SCALEPACK are available from Mac Science Co., Z. Otwinowski, University of Texas, Southwestern Medical Center. The program teXsan is available from Rigaku Co. The program SIR97 is available from <http://www.irmec.ba.cnr.it/>. The program SHELXL97 is available from <http://shelx.uni-ac.gwdg.de/SHELX/>. The program ORTEP-III is available from <http://www.ornl.gov/ortep/ortep.html>. All crystallographic data (excluding structure factors) for the compounds reported in this paper have been deposited with the Cambridge Crystallographic Data Centre (all data have each supplementary publication number). A copy of the data can be obtained free of charge on application to CCDC, 12 Union Road, Cambridge CB2 1EZ, UK (fax, (+44)1223-336-033; e-mail, deposit@ccdc.cam.ac.uk).

**1** (deposited as CCDC-186149):  $C_{17}H_{13}F_3O_5S$ , 386.34, triclinic,  $P\bar{1}$ , pale green,  $a = 8.5460(6)$  Å,  $b = 9.4300(8)$  Å,  $c = 11.1650(7)$  Å,  $\alpha = 73.016(4)^\circ$ ,  $\beta = 82.571(5)^\circ$ ,  $\gamma = 81.014(4)^\circ$ ,  $V = 846.6(1)$  Å<sup>3</sup>, 298 K,  $Z = 2$ ,  $R = 0.0532$ , GOF = 1.443.

**6** (deposited as CCDC-185971):  $C_{16}H_{14}O_2$ , 238.27, monoclinic,  $P2_1/c$ , pale yellow-green,  $a = 6.642(5)$  Å,  $b = 12.169(5)$  Å,  $c = 15.118(5)$  Å,  $\beta = 91.913(5)^\circ$ ,  $V = 1221.3(11)$  Å<sup>3</sup>, 298 K,  $Z = 4$ ,  $R = 0.0766$ , GOF = 1.160.

**9** (deposited as CCDC-186017):  $C_{20}H_{25}O_6P$ , 390.37, orthorhombic,  $P2_12_12_1$ , pale yellow-green,  $a = 10.0330(2)$  Å,  $b = 11.9530(5)$  Å,  $c = 16.2950(7)$  Å,  $V = 1954.2(1)$  Å<sup>3</sup>, 298 K,  $Z = 4$ ,  $R = 0.0514$ , GOF = 1.000.

**11** (deposited as CCDC-186150):  $C_{14}H_7Br_3$ , 414.92, monoclinic,  $P2_1/c$ , yellow,  $a = 10.1530(5)$  Å,  $b = 7.2480(2)$  Å,  $c = 17.3580(9)$  Å,  $\beta = 106.064(2)^\circ$ ,  $V = 1227.48(9)$  Å<sup>3</sup>, 130 K,  $Z = 4$ ,  $R = 0.0410$ , GOF = 1.041.

**23** (deposited as CCDC-186018):  $C_{15}H_{12}Br_2O$ , 368.07, orthorhombic,  $Pnma$ , yellow,  $a = 7.3340(3)$  Å,  $b = 19.5430(4)$  Å,  $c = 9.0820(4)$  Å,  $V = 1301.7(1)$  Å<sup>3</sup>, 298 K,  $Z = 4$ ,  $R = 0.0919$ , GOF = 1.481.

**25** (deposited as CCDC-186229):  $C_{17}H_{13}NO_2$ , 263.30, tetragonal,  $I4_1/a$ , yellow,  $a = 25.057(3)$  Å,  $c = 8.3710(5)$  Å,  $V = 5255.8(7)$  Å<sup>3</sup>, 298 K,  $Z = 16$ ,  $R = 0.0753$ , GOF = 1.478.

**27** (deposited as CCDC-186148):  $C_{19}H_{20}B_2F_7O_4$ , 466.97, monoclinic,  $P2_1/c$ , yellow,  $a = 10.981(2)$  Å,  $b = 14.701(4)$  Å,  $c = 13.430(3)$  Å,  $\beta = 107.81(2)^\circ$ ,  $V = 2064.2(8)$  Å<sup>3</sup>, 200 K,  $Z = 4$ ,  $R = 0.1047$ , GOF = 1.574.

**38** (deposited as CCDC-183680):  $C_{29}H_{31}F_6KO_8$ , 660.64, orthorhombic,  $Pbca$ , purple,  $a = 13.9100(3)$  Å,  $b = 19.2280(5)$  Å,  $c = 23.5150(7)$  Å,  $V = 6289.4(3)$  Å<sup>3</sup>, 150 K,  $Z = 8$ ,  $R = 0.1050$ , GOF = 1.939.

**50** (deposited as CCDC-176315):  $C_{24}H_{23}BN_2O_2$ , 382.27, monoclinic,  $P2_1/n$ , pale yellow,  $a = 16.3780(6)$  Å,  $b = 7.4670(2)$  Å,  $c = 16.9660(6)$  Å,  $\beta = 105.007(2)^\circ$ ,  $V = 2004.1(1)$  Å<sup>3</sup>, 298 K,  $Z = 4$ ,  $R = 0.0661$ , GOF = 1.308.

**51** (deposited as CCDC-176316):  $C_{20}H_{25}BN_2$ , 304.24, monoclinic,  $P2_1/n$ , pale yellow,  $a = 10.7260(4)$  Å,  $b = 12.5420(4)$  Å,  $c = 13.0800(4)$  Å,  $\beta = 91.437(2)^\circ$ ,  $V = 1759.04(9)$  Å<sup>3</sup>, 298 K,  $Z = 4$ ,  $R = 0.0699$ , GOF = 1.584.

**52** (deposited as CCDC-176317):  $C_{18}H_{19}BCl_2N_2$ , 345.08, monoclinic,  $P2_1/n$ , pale yellow,  $a = 12.7770(4)$  Å,  $b = 12.5510(6)$  Å,  $c = 10.7200(5)$  Å,  $\beta = 90.546(3)^\circ$ ,  $V = 1719.0(1)$  Å<sup>3</sup>, 298 K,  $Z = 4$ ,  $R = 0.0667$ , GOF = 1.516.

(50) Altomare, A.; Burla, M. C.; Camalli, M.; Casciaro, G. L.; Giacovazzo, C.; Guagliardi, A.; Moliterni, A. G. G.; Polidori, G.; Spagna, R. *J. Appl. Crystallogr.* **1999**, *32*, 115.

(51) Sheldrick, G. M. *SHELX-97, Program for the Refinement of Crystal Structures*; University of Göttingen: Göttingen, Germany, 1997.

(52) Burnett, M. N.; Johnson, C. K. *ORTEP-III: Oak Ridge Thermal Ellipsoid Plot Program for Crystal Structure Illustrations*; Oak Ridge National Laboratory Report ORNL-6895, 1996.

**56** (deposited as CCDC-141764):  $C_{22}H_{17}BO_4$ , 356.18, monoclinic,  $P2_1/a$ , pale blue-green,  $a = 11.9620(4)$  Å,  $b = 7.2280(1)$  Å,  $c = 20.2810(7)$  Å,  $\beta = 100.490(1)^\circ$ ,  $V = 1724.21(7)$  Å<sup>3</sup>, 298 K,  $Z = 4$ ,  $R = 0.0560$ , GOF = 1.367.

**57** (deposited as CCDC-141765):  $C_{23}H_{19}BO_5$ , 386.21, orthorhombic,  $Pca2_1$ , pale blue-green,  $a = 9.8670(4)$  Å,  $b = 14.2920(6)$  Å,  $c = 14.0810(4)$  Å,  $V = 1985.7(1)$  Å<sup>3</sup>,  $Z = 4$ ,  $R = 0.0570$ , GOF = 0.847.

**58** (deposited as CCDC-141766):  $C_{22}H_{17}BO_2S_2$ , 388.31, orthorhombic,  $Pnma$ , pale blue-green,  $a = 8.4930(2)$  Å,  $b = 14.3130(6)$  Å,  $c = 15.9540(8)$  Å,  $V = 1939.4(1)$  Å<sup>3</sup>, 298 K,  $Z = 4$ ,  $R = 0.0428$ , GOF = 1.438.

**59** (deposited as CCDC-185970):  $C_{18}H_{19}BO_4$ , 310.16, monoclinic,  $P2_1/n$ , pale blue-green,  $a = 18.7290(8)$  Å,  $b = 13.1770(5)$  Å,  $c = 21.8000(9)$  Å,  $\beta = 111.059(2)^\circ$ ,  $V = 5020.7(3)$  Å<sup>3</sup>, 298 K,  $Z = 12$ ,  $R = 0.0729$ , GOF = 1.681.

**60** (deposited as CCDC-185972):  $C_{16}H_{13}BF_2O_2$ , 286.08, orthorhombic,  $Pna2_1$ , pale blue-green,  $a = 12.1870(4)$  Å,  $b = 6.8230(2)$  Å,  $c = 32.524(1)$  Å,  $V = 2704.4(2)$  Å<sup>3</sup>, 298 K,  $Z = 8$ ,  $R = 0.0905$ , GOF = 1.459.

**61** (deposited as CCDC-185973):  $C_{16}H_{13}BCl_2O_2$ , 318.99, orthorhombic,  $Pmn2_1$ , yellow,  $a = 6.9500(2)$  Å,  $b = 9.0800(2)$  Å,  $c = 11.3230(4)$  Å,  $V = 714.55(4)$  Å<sup>3</sup>, 298 K,  $Z = 2$ ,  $R = 0.0625$ , GOF = 1.012.

**Experimental Electron Density Distribution Analysis of 56.** Single crystals of **56** were obtained by recrystallization from dichloromethane–*n*-hexane. The crystal having well-developed crystal faces,  $0.55 \times 0.49 \times 0.39$  mm<sup>3</sup>, was selected for the measurement. The diffraction data were collected on an automated imaging plate Weissenberg camera, Rigaku Raxis-Rapid, using Mo K $\alpha$  radiation ( $\lambda = 0.71073$  Å) generated from a fine focus sealed tube by an oscillation method at 100 K. To achieve high completeness, four data sets were measured with different crystal orientations. In each data set, 94 frames were measured with the oscillation angle  $2^\circ$  and interval  $1.5^\circ$  to form a total oscillation angle  $141.5^\circ$ . The Bragg spots on the imaging plates were integrated up to  $\sin \theta/\lambda = 1.2$  Å<sup>-1</sup> by the program PROCESS-AUTO.<sup>53</sup> The Lorentz and polarization corrections were applied during the integration processes. After application of absorption correction,<sup>54</sup> all 376 frames were scaled and averaged. Partial reflections were omitted in the scaling. The measured and independent reflections, completeness and  $R_{int}$  were 211351, 24835, 0.982 and 0.052, respectively. The structure was solved by a direct method and refined using independent 3836 reflections below  $\sin \theta/\lambda = 0.65$  Å<sup>-1</sup> with the programs SIR97<sup>50</sup> and SHELXL97,<sup>51</sup> respectively. Following the refinements, the high-order refinements were carried out using all 21 984 independent reflections with  $\sin \theta/\lambda \geq 0.6$  Å<sup>-1</sup> by the program SHELXL97. The positions of the hydrogen atoms were constrained to have C–H distances of 1.083 and 1.066 Å for the aromatic and methyl group, respectively.<sup>43a</sup> The refinements of the multipole expansion method using the Hansen–Coppens multipole

(53) PROCESS-AUTO; Rigaku Corporation: Tokyo, Japan, 1998.

(54) Higashi, T. NUMABS – Numerical Absorption Correction Based on Crystal Shape; Rigaku Corporation: Tokyo, Japan, 1999.

formalism<sup>55</sup> and topological analyses based on the resulting parameters were performed by the XD package.<sup>56</sup> The refinement was carried out against all the independent reflections of  $\sin \theta/\lambda \leq 1.2$  Å<sup>-1</sup> with  $I > 3\sigma(I)$  on  $F^2$ . At the first stage of the refinement, the atomic coordinates and the  $U_{ij}$  of non-hydrogen atoms were fixed on those of the high-order refinement, and the  $U_{iso}$  of the hydrogen atoms were fixed on those of the conventional refinement for the data below  $\sin \theta/\lambda = 0.65$  Å<sup>-1</sup>. The population parameters,  $P_v$ ,  $P_{lm\pm}$ , of non-hydrogen atoms and scale were refined. The level of the multipoles was raised stepwise up to hexadecapole for atoms B1, O1, and O2 and octupole for other non-hydrogen atoms. At the second stage, the anisotropic and isotropic temperature factors were refined for non-hydrogen and hydrogen atoms, respectively, followed by the refinements of the spherical Hartree–Fock radial screening parameter,  $\kappa$ , and isotropic extinction.<sup>57</sup> At the third stage, the  $P_v$ ,  $P_{lm\pm}$  and scale were refined. The level of the multipoles was raised to hexadecapole for atoms B1, O1, and O2, octupole for other non-hydrogen atoms, and dipole along the bond for hydrogen atoms in the same manner as in the first stage. After these refinements, the second and third strategies were repeated twice, and finally the  $P_v$ ,  $P_{lm\pm}$ ,  $\kappa$  coordinates and temperature factor of non-hydrogen atoms, isotropic extinction, and scale were refined. The number of parameters in the final cycle of the refinement was 742. A molecular electroneutrality constraint was applied through all the refinements. No significant peaks were found on the final residual maps. The residual maps in the planes of anthracene and catechol moieties, tables of the  $P_v$ ,  $P_{lm\pm}$ ,  $\kappa$  and  $F_o^2 - F_c^2$  and CIF file were deposited. Crystal data: monoclinic, space group  $P2_1/c$ ,  $a = 20.1411(2)$  Å,  $b = 7.1920(1)$  Å,  $c = 11.7510(1)$  Å,  $\beta = 100.8995(3)^\circ$ ,  $V = 1671.48(3)$  Å<sup>3</sup>,  $Z = 4$ ,  $D_x = 1.415$  g cm<sup>-3</sup>,  $R(F) = 0.0377$  (for 14 897 reflections with  $I > 3\sigma(I)$ ).

**Acknowledgment.** This work was supported by a Grant-in-Aid for Scientific Research (Nos. 09239103, 09440218, 11166248, 11304044, 12304044) provided by the Ministry of Education, Culture, Sports, Science and Technology of the Japanese Government and JSPS Research Fellowship (No. 08982) for Young Scientists. The authors are grateful to Central Glass Co., Ltd. for a generous gift of hexafluoroacetone trihydrate.

**Supporting Information Available:** All crystallographic data and CIF files. This material is available free of charge via the Internet at <http://pubs.acs.org>.

JA0438011

- (55) Hansen, N. K.; Coppens, P. *Acta Crystallogr., Sect. A*, **1978**, *34*, 909.  
 (56) Koritsanszky, T.; Howard, S.; Su, Z.; Mallinson, P. R.; Richter, T.; Hansen, N. K. *XD – a Computer Program Package for Multipole Refinement and Analysis of Electron Densities from Diffraction Data*; Free University of Berlin: Berlin, Germany.  
 (57) (a) Becker, P. J.; Coppens, P. *Acta Crystallogr., Sect. A*, **1974**, *30*, 129.  
 (b) Becker, P. J.; Coppens, P. *Acta Crystallogr., Sect. A*, **1975**, *31*, 417.